GPC3 Decreases IGF-1R–Grb10 Interaction and Promotes Cell Invasion in Hepatocellular Carcinoma in a Gender-Dependent Manner

Shu-Hsiang Liu
School of Nursing, National Taipei University of Nursing and Health Sciences, Taiwan
Po-Chun Huang
Institute of Biological Chemistry, Academia Sinica
Shiu-Ling Chen
Department of Applied Chemistry, National Chi-Nan University, Nantou, Taiwan
Tsai-Feng Fu
Department of Applied Chemistry, National Chi-Nan University, Nantou, Taiwan
Chun-Hsien Hsu
Center for Geriatrics and Gerontology, Department of Family Medicine, Department of Geriatric Medicine, Shin Kong Wu Ho-Su Memorial Hospital
Wuh-Liang Hwu
Institute of Biological Chemistry, Academia Sinica
Yu-May Lee
Institute of Biological Chemistry, Academia Sinica
Wei Cheng (kln8301@kln.mohw.gov.tw)
Department of Pathology, Kee-Lung Hospital, Ministry of Health and Welfare

Research Article

Keywords: glypican-3 (GPC3), insulin-like growth factor 1 receptor (IGF-1R), growth factor receptor-bound protein 10 (Grb10), hepatocellular carcinoma (HCC)

Posted Date: December 17th, 2020

DOI: https://doi.org/10.21203/rs.3.rs-124248/v1

Abstract

Background: Glypican-3 (GPC3) mRNA was more frequently overexpressed in women and patients with invasive HCC. We explore possible molecular mechanisms of the effect of GPC3 on growth factor receptor-bound protein 10 (Grb10) and insulin-like growth factor 1 receptor (IGF-1R) interaction of tumor invasion in women.

Methods: For *in vitro* experiments, GPC3 and pertinent mutants were transfected, and Western blotting (HEK293T cells), confocal microscopy (HeLa and PLC-PRF-5 cells), luciferase assays for AP-1 reporter activities (NIH3T3 and HuH-7 cells), gelatin zymography (PLC-PRF-5 cells) and cell culture in 3D collagen I gels (NIH3T3 and R- cells) were performed. For *in vivo* experiments, GPC3 and IGF-1R coexpression was evaluated in hepatocellular carcinoma clinical samples.

Results: We found that interaction of IGF-1R with Grb10 was hindered by GPC3, and GPC3 causes IGF-1R colocalization with Grb10 to a lesser extent after IGF-1 stimulation; moreover, it **promoted IGF-1-stimulated AP-1 activation and** matrix metalloproteinase -2 and 9 (MMP-2 and MMP-9) secretion *in vitro*, which seemingly play a role in tumor invasion or recurrence. Further, gender differences existed among patients with hepatocellular carcinoma in terms of GPC3 and IGF-1R coexpression *in vivo*.

Conclusions: We believe that a more intensive surveillance of GPC3 expression in female patients with hepatocellular carcinoma should contribute to the prediction of recurrence, and this may highlight new strategies for treating hepatocellular carcinoma in women.

Introduction

Hepatocellular carcinoma (HCC) is the second leading cause of death due to malignancy worldwide (1). Gender differences in the incidence of HCC are evident, with the male:female ratio ranging from 2:1 to 4:1 (2, 3). Gender differences have also been reported in HCC recurrence among recipients of a liver transplant (LT), with the incidence being nearly three times higher in women than in men among those with high α-fetoprotein (AFP) levels at the time of transplantation (4). We previously reported that glypican-3 (GPC3) mRNA was more frequently overexpressed in women and patients with invasive HCC (5), demonstrating that higher levels of insulin-like growth factor 1 (IGF-1) receptor (IGF-1R) were found in GPC3-expressing cells because GPC3 decreased IGF-1-induced IGF-1R ubiquitination and degradation (6).

Glypicans are a family of heparan sulfate proteoglycans linked to the exocytoplasmic surface of the plasma membrane by a glycosylphosphatidylinositol anchor (7). Glypicans act as coreceptors, facilitating the formation of ligand–receptor complexes and effectively lowering the required concentration of ligands (8). Loss-of-function mutations in GPC3 cause Simpson–Golabi–Behmel syndrome, a condition that is characterized by prenatal and postnatal overgrowth and an increased risk of embryonal tumor development (9). Studies have also demonstrated that GPC3 plays a key role in cancer development (7, 10, 11). GPC3 regulates the signaling activity of various morphogens, including Wnts, Hedgehogs, bone morphogenetic proteins and fibroblast growth factors (12–14). GPC3 reportedly

promotes the *in vitro* and *in vivo* growth of HCC cells by interacting with the Wnt ligand to facilitate Wnt/Frizzled binding (10). Furthermore, GPC3 seems to be both a serum marker (15) and a therapeutic target for HCC (16–18).

We previously demonstrated that GPC3 binds to IGF-2 and IGF-1R through its N-terminal proline-rich domain, causes the phosphorylation of IGF-1R and extracellular signal-regulated kinase (ERK) and induces oncogenicity (11). Further, GPC3 enhances IGF-1R signaling, leading to ERK phosphorylation, c-Myc expression and increased oncogenicity (6). GPC3 binds to and potentially sequesters growth factor receptor-bound protein 10 (Grb10), thereby blocking IGF-1R ubiquitination and degradation in the proteasome. Given that GPC3 is located in chromosome Xq26 and is more frequently overexpressed in women and patients with invasive HCC (5), we herein further investigated whether IGF-1R is associated with the mechanism of invasion by GPC3 and whether gender differences exist in GPC3 and IGF-1R coexpression in HCC.

Materials And Methods

Tissues and cells

Surgically resected liver tissue specimens were obtained from the Department of Pathology, National Taiwan University Hospital and Keelung Hospital, Ministry of Health and Welfare. These specimens were used in accordance with appropriate regulations and with approval by the Institutional Review Board of the Ethics Committees of the NTUH (200701095R) and KLH (TYGH100038). The HCC cell lines used were PLC-PRF-5 (CRL-8024) cells, which were purchased from ATCC (VA, USA), and HuH-7 cells (JCRB-0403) (19), which were from JCRB (Osaka, Japan). HEK293 (CRL-1573) and HEK293T cells were obtained from ATCC (CRL-3216). Prior to use, reauthentication of these cells was performed by Short Tandem Repeat (STR) DNA profiling analysis. NIH3T3 cells (BCRC-60008) were purchased from BCRC in 2003 (Hsinchu, Taiwan); NIH3T3 is a nonhuman cell line, and the morphology and growth speed of these cells have not changed since we obtained them (data not shown). HEK293T and NIH3T3 cells were used for transient transfection and stable clone selection. HeLa cells (BCRC-60005), which were authenticated through STR DNA profiling analysis, were purchased from BCRC in 2014. They were used for immunofluorescence staining within 6 months of cell resuscitation. Cells were cultured in Dulbecco's modified Eagle's medium supplemented with 10% fetal calf serum. G-418 (Promega, Fitchburg, WI, USA) was used for the selection of stable clones.

Plasmids and constructs

The wild-type GPC3 expression vector GPC3, convertase-resistant mutant RR→AA (11), proline residue mutant P26-30A, 70–453 a.a. deleted GPC3 expression vector (ΔGPC3), Grb10 and neural precursor cell-expressed developmentally downregulated 4 (Nedd4) have all been previously described (6). Activator protein-1 (AP-1) luciferase reporter was purchased from Promega (USA).

Antibodies and immune assays

The antibodies used in the present study included anti-GPC3 (1G12, Santa Cruz Biotechnology, Santa Cruz, CA, USA), anti-IGF1Rβ (#3027, Cell Signaling Technology, Danvers, MA, USA) (6), anti-Grb10 (Santa Cruz Biotechnology), anti-Flag (Institute of Biological Chemistry, Academia Sinica, Taipei, Taiwan) and anti-HA (New England Biolabs, Ipswich, MA, USA). Paraffin-embedded tissue sections were deparaffinized, and immunochemical staining was performed after antigen retrieval. Endogenous peroxidase activity was blocked with EnVision FLEX Peroxidase-Blocking Reagent (Dako, Agilent). For Western blot analyses, tissues and cells were extracted with HNTG buffer (20 mM HEPES buffer, pH 7.5; 150 mM NaCl; 0.1% Triton X-100; and 10% glycerol). Immunoprecipitation was performed by treating 0.5–1 mg of the cell lysate with HNTG buffer containing antibodies, and precipitated proteins were subsequently subjected to Western blotting.

Confocal microscopy

After transfection, cells were cultured in a serum-free medium, stained with IGF-1R (CD221, ThermoFisher, USA) antibody and stimulated with 50 ng/ml of IGF-1 for 10 min. They were then treated with 0.5% Triton X, fixed in 4% paraformaldehyde and stained with anti-Grb10 (Santa Cruz Biotechnology). The secondary antibodies were conjugated with Alexa 488 (green) for IGF-1R and Alexa 594 (red) for Grb10, and images were captured using a confocal laser scanning microscope.

Cell culture in 3D collagen I gels

We added the desired amount of collagen I (Corning, 354249) to obtain a final collagen I concentration of 2.3 mg/ml in a solution containing 10% 10 × minimal essential medium, 1% fetal calf serum (Sigma-Aldrich), and distilled water. The pH was adjusted to 7.4 with 1 N NaOH. Cells (2.5×10^5 cells/ml) were added to the aforementioned solution before it solidified. The mixture was then immediately transferred to a 96-well plate and allowed to solidify at 37 °C. After 30 min, 100 μl of normal complete culture medium was added on top of the cells and the collagen I gel mixture. Cells were cultured in the 3D collagen I gel for 3 d.

Luciferase assays for AP-1 reporter activities

Cells were transiently transfected with a combination of plasmids, as described in the legend of Fig. 4. After overnight transfection, they were treated with serum-free media for 48 h. Firefly luciferase (Promega) and Renilla luciferase (Applied Biosystems) assays were performed according to manufacturer instructions. For each experiment, transfections were performed in triplicate. Values represent means ± SD of at least three independent experiments. All values were normalized for transfection efficiency (Renilla luciferase activity).

Gelatin zymography

PLC-PRF-5 cells were cultured in serum-free medium for 3 d. The conditioned media with 8 μg of protein–after spin concentration–was mixed with nonreducing sodium dodecyl sulfate gel sample buffer and applied without boiling to a 10% polyacrylamide gel containing 0.1% sodium dodecyl sulfate and

1 mg/ml gelatin solution. After electrophoresis, the gels were washed with 50 mmol/l Tris-HCl (pH 7.5) containing 0.15 mol/l NaCl, 5 mmol/l $CaC1_2$, 5 µmol/l ZnCl, 0.02% NaN_3 and 0.25% Triton X-100 (three changes) at room temperature and then incubated in the same buffer without Triton X-100 (two changes) at 37 °C for 20 h. Proteins were stained with Coomassie Brilliant Blue R-250.

Results

Gender differences in the coexpression of GPC3 and IGF-1R in HCC

We previously found that GPC3 mRNA was more frequently overexpressed in female than in male patients with HCC (5) and later confirmed this finding through an immunohistochemistry study (6), wherein we observed that GPC3 expression was highly correlated with IGF-1R expression in HCC specimens (6). Herein, we studied 126 patients with HCC (98 men and 28 women) to determine if gender differences are evident in GPC3 and IGF-1R coexpression. GPC3 expression was observed more frequently in women than in men (Fig. 1A and B, 92.8% vs. 52%), and GPC3 and IGF-1R coexpression was found to be correlated with gender (Table 1 and Fig. 1C, p = 0.0001 by Fisher's exact test). Interestingly, GPC3 and IGF-1R were more often coexpressed in women (100%) than in men (57.1%), with AFP levels > 320 ng/ml (5).

Table 1
IHC results of the HCC clinical samples

	IHC results				
Gender	GPC3+/IGF-1R+	GPC3+/IGF-1R-	GPC3-/IGF-1R+	GPC3-/IGF-1R-	total
female n (%)	24 (85.7%)	2 (7.1%)	0	2 (7.1%)	28 (100%)
male n (%)	38 (38.7%)	13 (13.3%)	20 (20.4%)	27 (27.6%)	98 (100%)

Less interaction between Nedd4, Grb10 and IGF-1R in the presence of GPC3

We previously demonstrated that GPC3 coimmunoprecipitated with Grb10 but not with Nedd4 (6). Herein we stimulated HCC cells with IGF-1 and found that GPC3 decreased the ability of Grb10 to pull down IGF-1R by approximately 0.5-fold (Fig. 2, lane 4). Nedd4 also weakly bound to Grb10 in GPC3-expressing cells stimulated with IGF-1 (Fig. 2, lane 4). It is therefore likely that GPC3 bound to and sequestered Grb10, thereby preventing its binding to IGF-1R. In HeLa and PLC-PRF-5 cells, IGF-1R was internalized to a lesser extent and was colocalized with Grb10 after stimulating GPC3-expressing cells with IGF-1 (Fig. 3A and 3B). As control, IGF-1R was colocalized with Grb10 in the presence of the GPC3 mutant P26-30A (the

GPC3 mutant cannot bind to IGF-1R or be internalized and colocalized with Grb10 after IGF-1 stimulation; Fig. 3A) or vector control (Fig. 3A and 3B) upon stimulation with IGF-1.

ΔGPC3 prevented IGF-1-stimulated AP-1 activation

IGF-1 is known to activate AP-1 and its downstream genes in response to extracellular stimuli (20, 21). Using an AP-1 luciferase reporter, we demonstrated that GPC3 overexpression increased luciferase activity in NIH3T3 cells by up to 2.5-fold in serum-free conditions. Moreover, IGF-1 treatment further increased the luciferase activity in GPC3-overexpressing NIH3T3 cells, suggesting that the effects of GPC3 and IGF-1 are additive (Fig. 4A). HuH-7 cells expressed high levels of endogenous GPC3, and therefore, the effect of GPC3 overexpression on AP-1 activity was minimal (Fig. 4B). By inducing the expression of ΔGPC3 (the deleted GPC3 mutant cannot protect IGF-1R from degradation) in HuH-7 cells, we demonstrated that ΔGPC3 not only decreased the basal levels of AP-1 activity in the cells but also inhibited the effects of IGF-1 stimulation (Fig. 4B).

GPC3 increased MMP-2 and MMP-9 expression

We previously found GPC3 mRNA was more frequently overexpressed in invasive HCC (5). The AP-1 binding site is reportedly a direct regulator of MMP activity (22),, which is critical for the invasive potential of tumors and is a predictor of tumor recurrence and survival in patients with HCC after surgical resection (23). Increased production of MMP-2 has been observed in cells overexpressing IGF-1R (24) and via the phosphoinositide 3-kinase (PI3-K) and mitogen-activated protein kinase (MAPK) pathways (25). Therefore, we herein assessed whether GPC3 induces MMP-2 and MMP-9 expression.

In the case of PLC-PRF-5 cells, more MMP-2 and MMP-9 were found in the conditioned media of GPC3-expressing cells than in the conditioned media of the vector control or GPC3 mutant cells (Fig. 5A). In addition, more activated ERK was found in PLC-PRF-5 cells expressing GPC3 than in the vector control or GPC3 mutant cells (Fig. 5B). Similarly, increased p-ERK expression was observed in GPC3-expressing NIH3T3 cells (Fig. 6A), and 3D collagen I gels exhibited more invasive outgrowth with dramatic invadopodia (Fig. 6C). By contrast, GPC3 did not activate ERK (Fig. 6B) or promote the outgrowth of invadopodia in R-cells (IGF-1R knockout mouse embryonal fibroblasts; Fig. 6D). These observations suggest that GPC3 plays a role in the promotion of invasive properties through IGF-1R.

Discussion

In this study, we demonstrated that GPC3 causes IGF-1R colocalization with Grb10 to a lesser extent after IGF-1 stimulation and it promotes more IGF-1-stimulated activation of AP-1 and more secretion of both MMP-2 and MMP-9, all of which may play a role in tumor invasion or recurrence. In addition, gender differences were evident in GPC3 and IGF-1R coexpression in HCC clinical samples.

GPC3 was also found to decrease the ability of Grb10 to pull down IGF-1R and Nedd4 (an E3 ubiquitin ligase). Similar findings have been reported for another E3 ligase, namely MDM2, which was observed to

bind to isoforms of p73 (TAp73α and ΔNp73α) and to a much lesser extent to isoforms of p63 (TAp63α and ΔNp63α). Further, MDM2 was noted to inhibit the transcriptional activity of the isoforms of p73 but to have almost no effect on those of p63 (26). Therefore, less IGF-1R interaction with Grb10 and Nedd4 caused by GPC3 seems to protect IGF-1R from degradation and enhance IGF-1R signaling.

The extracellular MMP-9 and MMP-2 are critical for the invasive potential of tumors and for the prediction of tumor recurrence and survival in patients with HCC after surgical resection (23). In the prostate cancer cell line DU145, IGF-1 has been shown to regulate MMP-2 and MMP-9 activity and expression via the PI3-K and MAPK pathways, and the invasive capacity of DU145 cells was inhibited by blocking IGF-1R (25). In GPC3-expressing cells, increased levels of IGF-1R, p-ERK, MMP-2 and MMP-9 and higher invasive capacity were found. By contrast, the invasive capacity or ERK activation of GPC3 was eliminated in IGF-1R knockout R-cells. Therefore, IGF-1R is clearly essential for GPC3-induced invasion.

In the present study as well as in previous studies, GPC3 and IGF-1R were found to be more frequently coexpressed in female patients with HCC; moreover, gender differences regarding their role in HCC were statistically significant. GPC3 was more frequently overexpressed in women and closely correlated with elevation of serum AFP levels (5). IGF-1R mediates cancer invasion (27), and risk of tumor recurrence (28). HCC recurrence in LT recipients was reported to be nearly three times higher in women than in men with high AFP levels (> 100 ng/dl) at LT (4), and this correlates the finding of gender differences in the coexpression of GPC3 and IGF-1R in HCC samples with high AFP levels in this study.

In conclusion, we found evidence of gender differences in the coexpression of GPC3 and IGF-1R in HCC and that GPC3-expressing HCC cells exhibit higher MMP-2 and MMP-9 secretion. Considering that such substantial gender differences exist in HCC in terms of GPC3 expression and its effects, a subset of female patients with HCC may benefit from more intensive surveillance of GPC3 expression. Different strategies to target GPC3 for the effective treatment of HCC in women are at present in development.

Abbreviations

glypican-3 (GPC3); insulin-like growth factor 1 receptor (IGF-1R); growth factor receptor-bound protein 10 (Grb10); hepatocellular carcinoma (HCC)

Declarations

Ethics approval

The human tissue involved in the study were de-linked and approved by Institutional Review Board of the Ethics Committees of the NTUH (200701095R) and KLH (TYGH100038). There was no animal study. All methods were carried out in accordance with relevant guidelines and regulations.

Consent for publication

Not applicable.

Availability of data and material

The datasets generated during and/or analyzed during the current study are available from the corresponding author on reasonable request.

Competing Interests

None declared.

Funding

This work was supported by Kee-Lung Hospital, Ministry of Health and Welfare (106-01 and 107-01 to Wei Cheng).

Authors' contributions

LSH and LYM investigated and supervised the findings of this work. HPC, CSL, FTF, HCH and HWL collected the data and analysis. The corresponding author CW conceived the present idea, wrote the manuscript, takes primary responsibility for communication with the journal and editorial office during the submission process, throughout peer review and during publication.

Acknowledgements

We thank Ms. Hsin-Lun Liu for her valuable technical assistance. This manuscript was edited by Wallace Academic Editing.

References

1. Mazzanti R, Arena U, Tassi R. Hepatocellular carcinoma: Where are we? World J Exp Med. 2016 Feb 20;6(1):21–36.
2. El-Serag HB, Rudolph KL. Hepatocellular carcinoma: epidemiology and molecular carcinogenesis. Gastroenterology. 2007 Jun;132(7):2557–76.
3. Sarkar M, Watt KD, Terrault N, Berenguer M. Outcomes in liver transplantation: does sex matter? J Hepatol. 2015 Apr;62(4):946–55.
4. Sarkar M, Dodge JL, Roberts JP, Terrault N, Yao F, Mehta N. Increased hepatocellular carcinoma recurrence in women compared to men with high alpha fetoprotein at liver transplant. Ann Hepatol. 2016 Jul-Aug;15(4):545–9.
5. Hsu HC, Cheng W, Lai PL. Cloning and expression of a developmentally regulated transcript MXR7 in hepatocellular carcinoma: biological significance and temporospatial distribution. Cancer Res. 1997 Nov 15;57(22):5179–84.

6. Cheng W, Huang PC, Chao HM, Jeng YM, Hsu HC, Pan HW, et al. Glypican-3 induces oncogenicity by preventing IGF-1R degradation, a process that can be blocked by Grb10. Oncotarget. 2017 Jul;8:80429–42.
7. Filmus J, Selleck SB. Glypicans: proteoglycans with a surprise. J Clin Invest. 2001 Aug;108(4):497–501.
8. Fuster MM, Esko JD. The sweet and sour of cancer: glycans as novel therapeutic targets. Nat Rev Cancer. 2005 Jul;5(7):526–42.
9. Pilia G, Hughes-Benzie RM, MacKenzie A, Baybayan P, Chen EY, Huber R, et al. Mutations in GPC3, a glypican gene, cause the Simpson-Golabi-Behmel overgrowth syndrome. Nat Genet. 1996 Mar;12(3):241–7.
10. Capurro MI, Xiang YY, Lobe C, Filmus J. Glypican-3 promotes the growth of hepatocellular carcinoma by stimulating canonical Wnt signaling. Cancer Res. 2005 Jul 15;65(14):6245–54.
11. Cheng W, Tseng CJ, Lin TT, Cheng I, Pan HW, Hsu HC, et al. Glypican-3-mediated oncogenesis involves the Insulin-like growth factor-signaling pathway. Carcinogenesis. 2008 Jul;29(7):1319–26.
12. De Cat B, Muyldermans SY, Coomans C, Degeest G, Vanderschueren B, Creemers J, et al. Processing by proprotein convertases is required for glypican-3 modulation of cell survival, Wnt signaling, and gastrulation movements. J Cell Biol. 2003 Nov 10;163(3):625–35.
13. Capurro MI, Xu P, Shi W, Li F, Jia A, Filmus J. Glypican-3 inhibits Hedgehog signaling during development by competing with patched for Hedgehog binding. Dev Cell. 2008 May;14(5):700–11.
14. Grisaru S, Cano-Gauci D, Tee J, Filmus J, Rosenblum ND. Glypican-3 modulates BMP- and FGF-mediated effects during renal branching morphogenesis. Dev Biol. 2001 Mar 1;231(1):31–46.
15. Jia XB, Gao YT, Zhai DK, Liu J, Ca J, Wang YJ, et al. Assessment of the Clinical Utility of Glypican 3 as a Serum Marker for the Diagnosis of Hepatocellular Carcinoma. Technology in Cancer Research & Treatment. 2016;15(6):780–6.
16. Wang L, Yao M, Pan LH, Qian Q, Yao DF. Glypican-3 is a biomarker and a therapeutic target of hepatocellular carcinoma. Hepatobiliary Pancreat Dis Int. 2015 Aug;14(4):361–6.
17. Filmus J, Capurro M. Glypican-3: a marker and a therapeutic target in hepatocellular carcinoma. FEBS J. 2013 May;280(10):2471–6.
18. Haruyama Y, Kataoka H. Glypican-3 is a prognostic factor and an immunotherapeutic target in hepatocellular carcinoma. World J Gastroenterol. 2016 Jan 7;22(1):275–83.
19. Nakabayashi H, Taketa K, Miyano K, Yamane T, Sato J. Growth of human hepatoma cells lines with differentiated functions in chemically defined medium. Cancer Res. 1982 Sep;42(9):3858–63.
20. Karin M. The regulation of AP-1 activity by mitogen-activated protein kinases. J Biol Chem. 1995 Jul 14;270(28):16483–6.
21. Hadsell DL, Abdel-Fattah G. Regulation of cell apoptosis by insulin-like growth factor I. Adv Exp Med Biol. 2001;501:79–85.

22. Benbow U, Brinckerhoff CE. The AP-1 site and MMP gene regulation: what is all the fuss about? Matrix Biol. 1997 Mar;15(8–9):519–26.
23. Chen R, Cui J, Xu C, Xue T, Guo K, Gao D, et al. The significance of MMP-9 over MMP-2 in HCC invasiveness and recurrence of hepatocellular carcinoma after curative resection. Ann Surg Oncol. 2012 Jul;19 Suppl 3:S375-84.
24. Long L, Navab R, Brodt P. Regulation of the Mr 72,000 type IV collagenase by the type I insulin-like growth factor receptor. Cancer Res. 1998 Aug 1;58(15):3243-7.
25. Saikali Z, Setya H, Singh G, Persad S. Role of IGF-1/IGF-1R in regulation of invasion in DU145 prostate cancer cells. Cancer Cell Int. 2008 Jul 3;8:10.
26. Stindt MH, Muller PA, Ludwig RL, Kehrloesser S, Dotsch V, Vousden KH. Functional interplay between MDM2, p63/p73 and mutant p53. Oncogene. 2015 Aug 13;34(33):4300-10.
27. Kucab JE, Dunn SE. Role of IGF-1R in mediating breast cancer invasion and metastasis. Breast Dis. 2003;17:41–7.
28. Aleksic T, Verrill C, Bryant RJ, Han C, Worrall AR, Brureau L, et al. IGF-1R associates with adverse outcomes after radical radiotherapy for prostate cancer. Br J Cancer. 2017 Nov 21;117(11):1600-6.

Figures

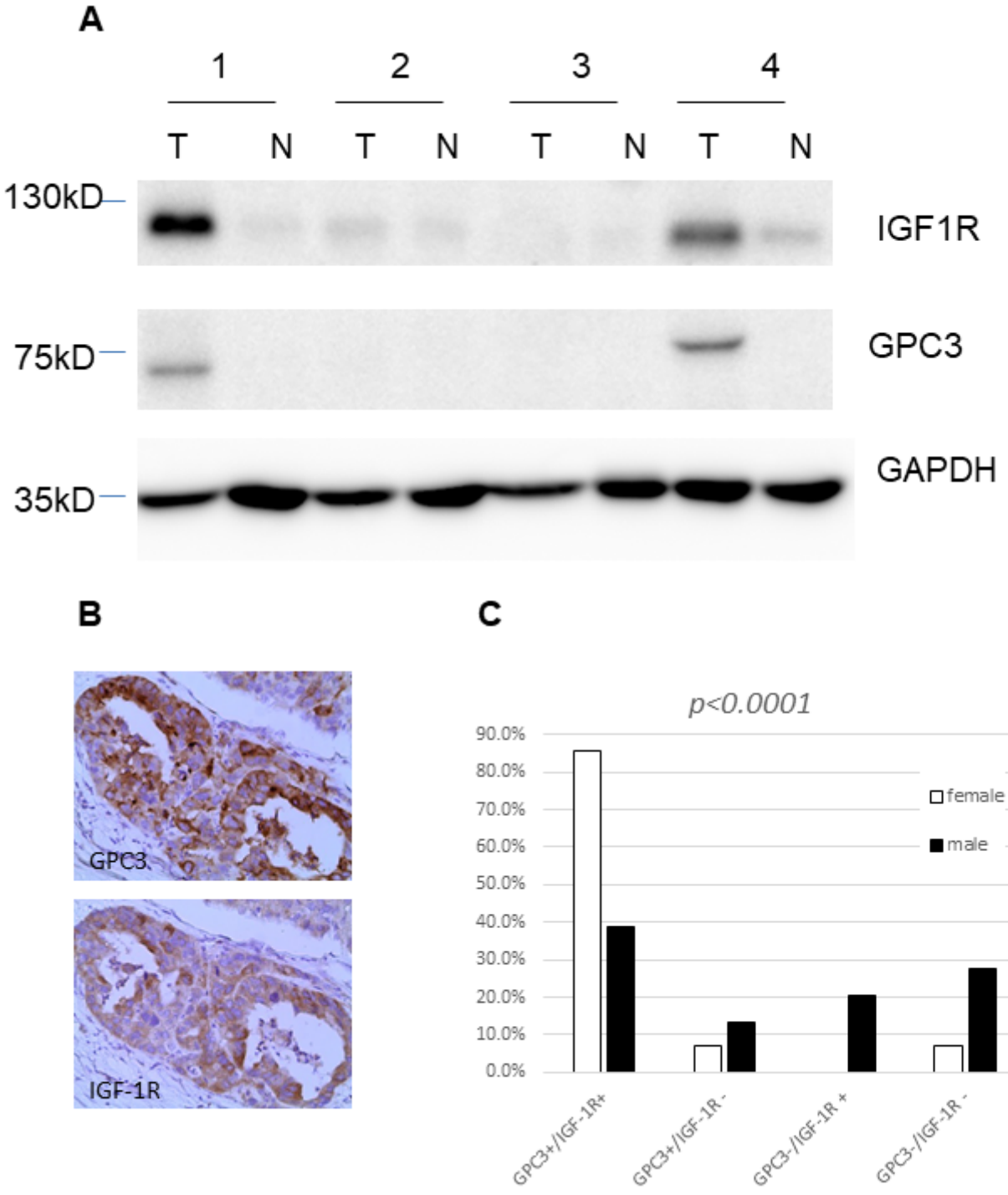

Figure 1

Gender-related differences in the expression of GPC3 and IGF-1R in HCC. (A) Western blot analysis of IGF-1R and GPC3 in tumor (T) and nontumor (N) parts of HCC. GAPDH was used as the loading control. Full blots with molecular weight markers are shown in Supplementary Figure S1. (B) Immunohistochemistry of GPC3 and IGF-1R HCC specimens exhibited positive GPC3 and IGF-1R staining in the tumor regions (200×). (C) Correlation between GPC3 and IGF-1R coexpression and gender in 126 HCC cases. The p value was determined using Fisher's exact test.

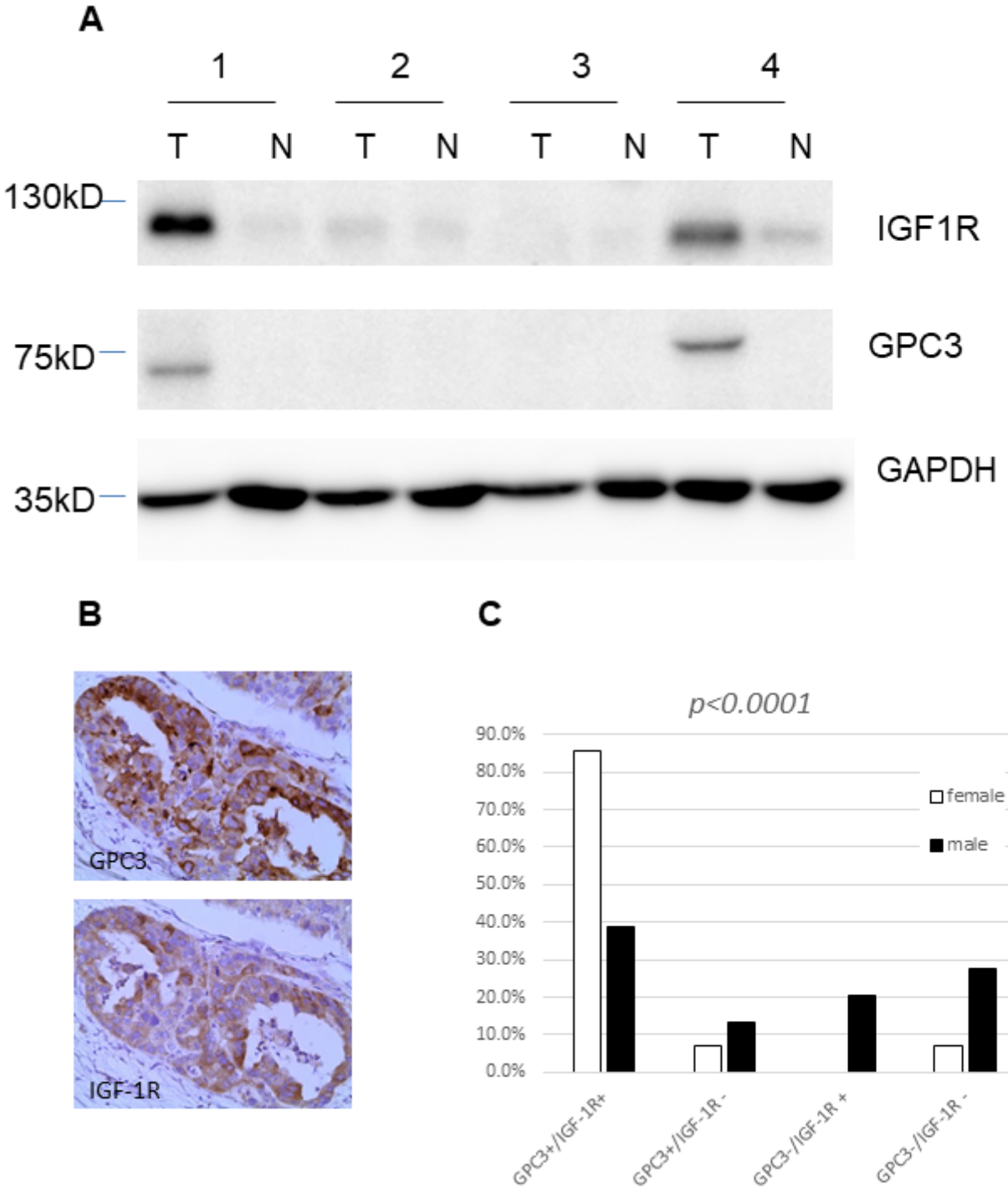

Figure 1

Gender-related differences in the expression of GPC3 and IGF-1R in HCC. (A) Western blot analysis of IGF-1R and GPC3 in tumor (T) and nontumor (N) parts of HCC. GAPDH was used as the loading control. Full blots with molecular weight markers are shown in Supplementary Figure S1. (B) Immunohistochemistry of GPC3 and IGF-1R HCC specimens exhibited positive GPC3 and IGF-1R staining in the tumor regions (200×). (C) Correlation between GPC3 and IGF-1R coexpression and gender in 126 HCC cases. The p value was determined using Fisher's exact test.

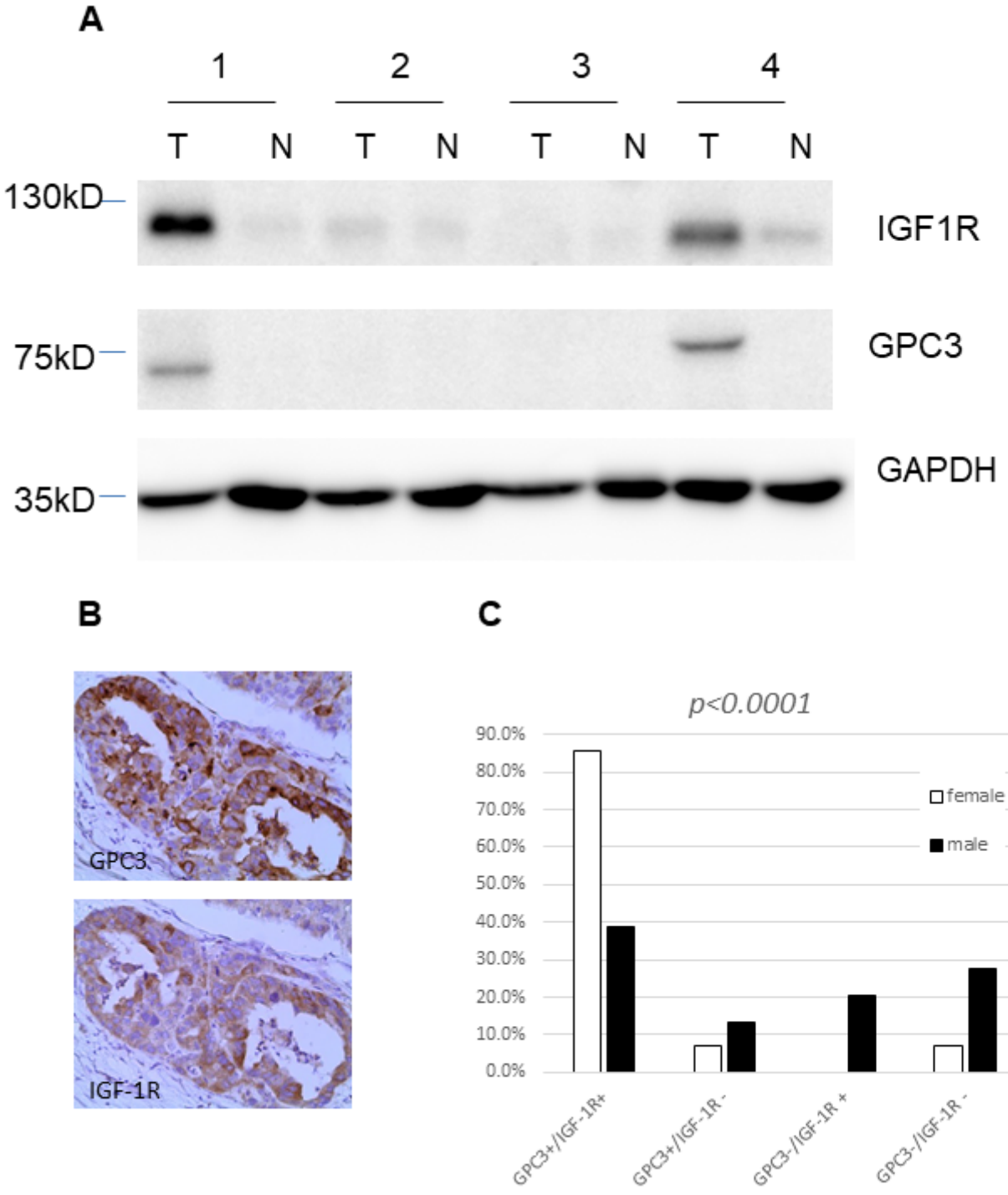

Figure 1

Gender-related differences in the expression of GPC3 and IGF-1R in HCC. (A) Western blot analysis of IGF-1R and GPC3 in tumor (T) and nontumor (N) parts of HCC. GAPDH was used as the loading control. Full blots with molecular weight markers are shown in Supplementary Figure S1. (B) Immunohistochemistry of GPC3 and IGF-1R HCC specimens exhibited positive GPC3 and IGF-1R staining in the tumor regions (200×). (C) Correlation between GPC3 and IGF-1R coexpression and gender in 126 HCC cases. The p value was determined using Fisher's exact test.

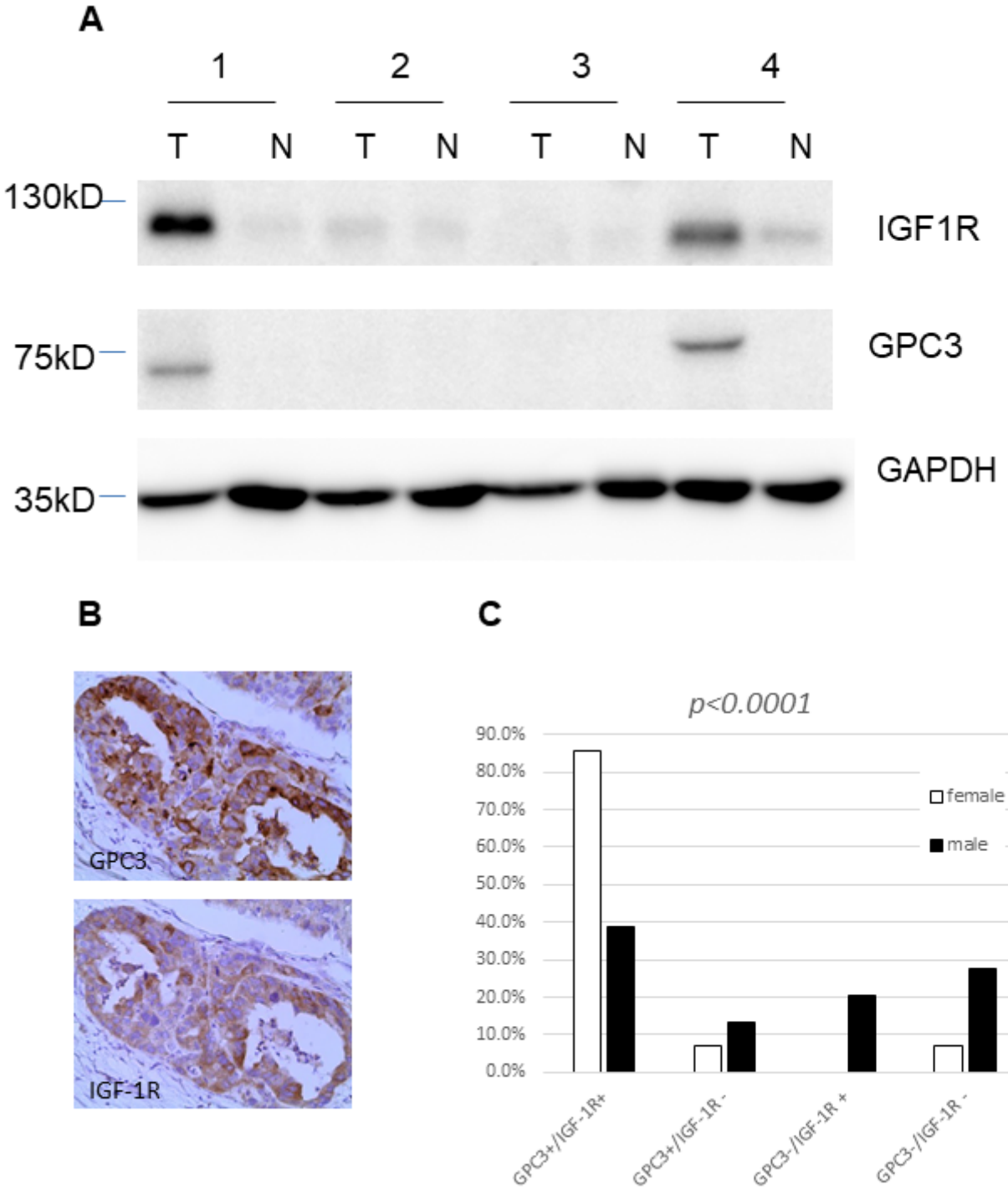

Figure 1

Gender-related differences in the expression of GPC3 and IGF-1R in HCC. (A) Western blot analysis of IGF-1R and GPC3 in tumor (T) and nontumor (N) parts of HCC. GAPDH was used as the loading control. Full blots with molecular weight markers are shown in Supplementary Figure S1. (B) Immunohistochemistry of GPC3 and IGF-1R HCC specimens exhibited positive GPC3 and IGF-1R staining in the tumor regions (200×). (C) Correlation between GPC3 and IGF-1R coexpression and gender in 126 HCC cases. The p value was determined using Fisher's exact test.

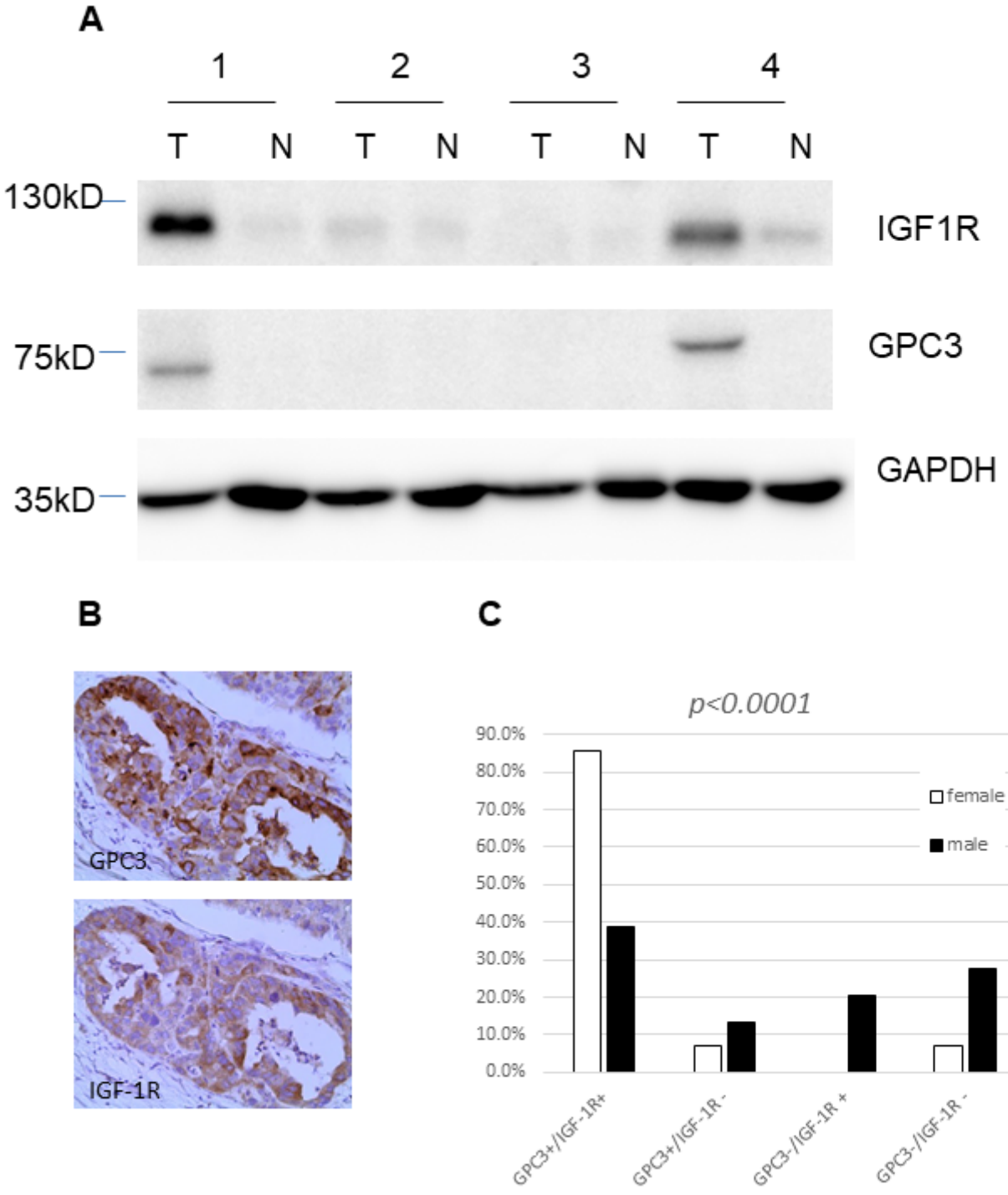

Figure 1

Gender-related differences in the expression of GPC3 and IGF-1R in HCC. (A) Western blot analysis of IGF-1R and GPC3 in tumor (T) and nontumor (N) parts of HCC. GAPDH was used as the loading control. Full blots with molecular weight markers are shown in Supplementary Figure S1. (B) Immunohistochemistry of GPC3 and IGF-1R HCC specimens exhibited positive GPC3 and IGF-1R staining in the tumor regions (200×). (C) Correlation between GPC3 and IGF-1R coexpression and gender in 126 HCC cases. The p value was determined using Fisher's exact test.

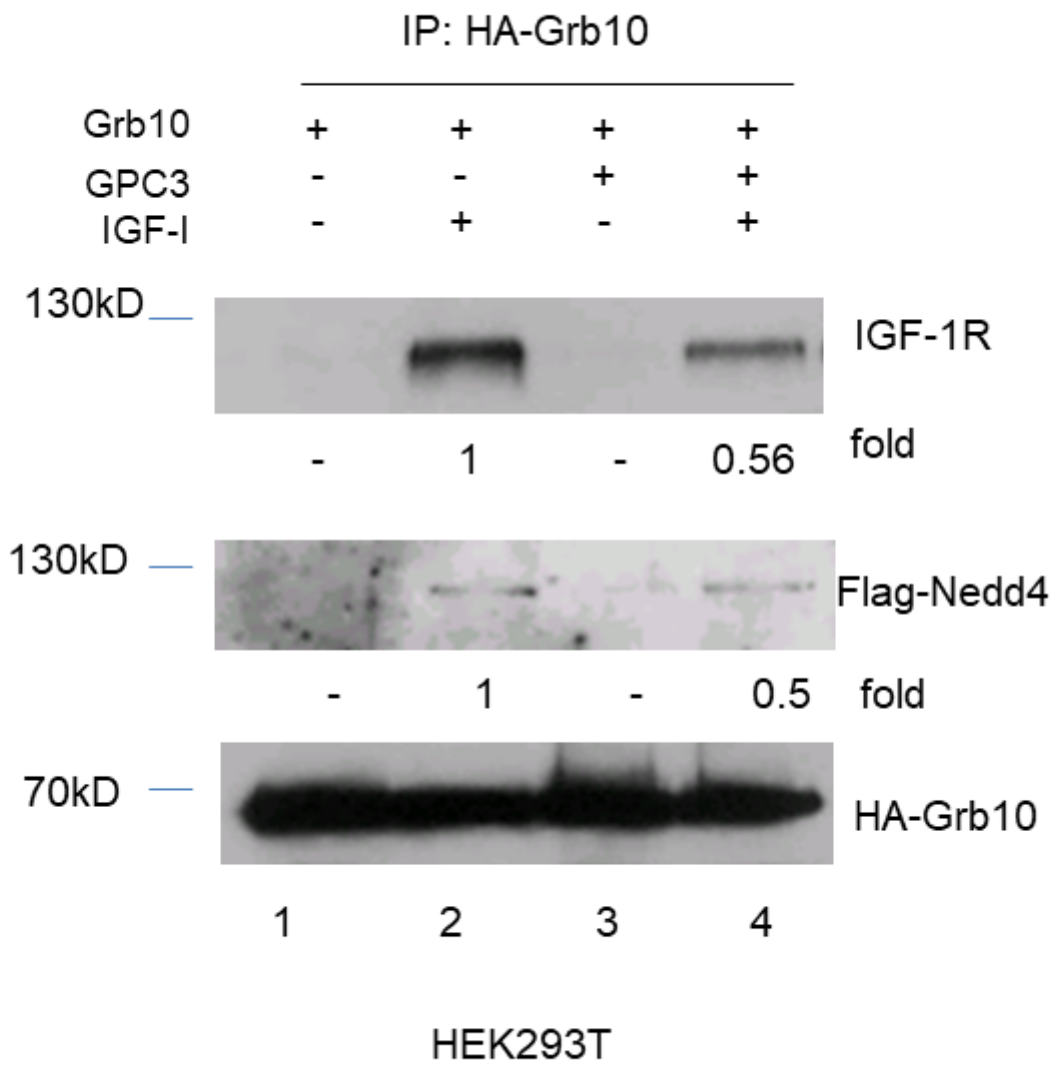

Figure 2

Less interaction between Grb10 and IGF-1R occurred in the presence of GPC3. HEK293T cells were transfected with expression vectors and stimulated with IGF-1 for 5 min. After immunoprecipitation with an anti-HA affinity matrix, IGF-1R bound to HA-Grb10 only in the presence of IGF-1 (Panel 1, lanes 2 and 4); less IGF-1R bound to HA-Grb10 in the presence of GPC3 after IGF-1 stimulation (Panel 1, lane 4). Full blots with molecular weight markers are shown in Supplementary Figure S2.

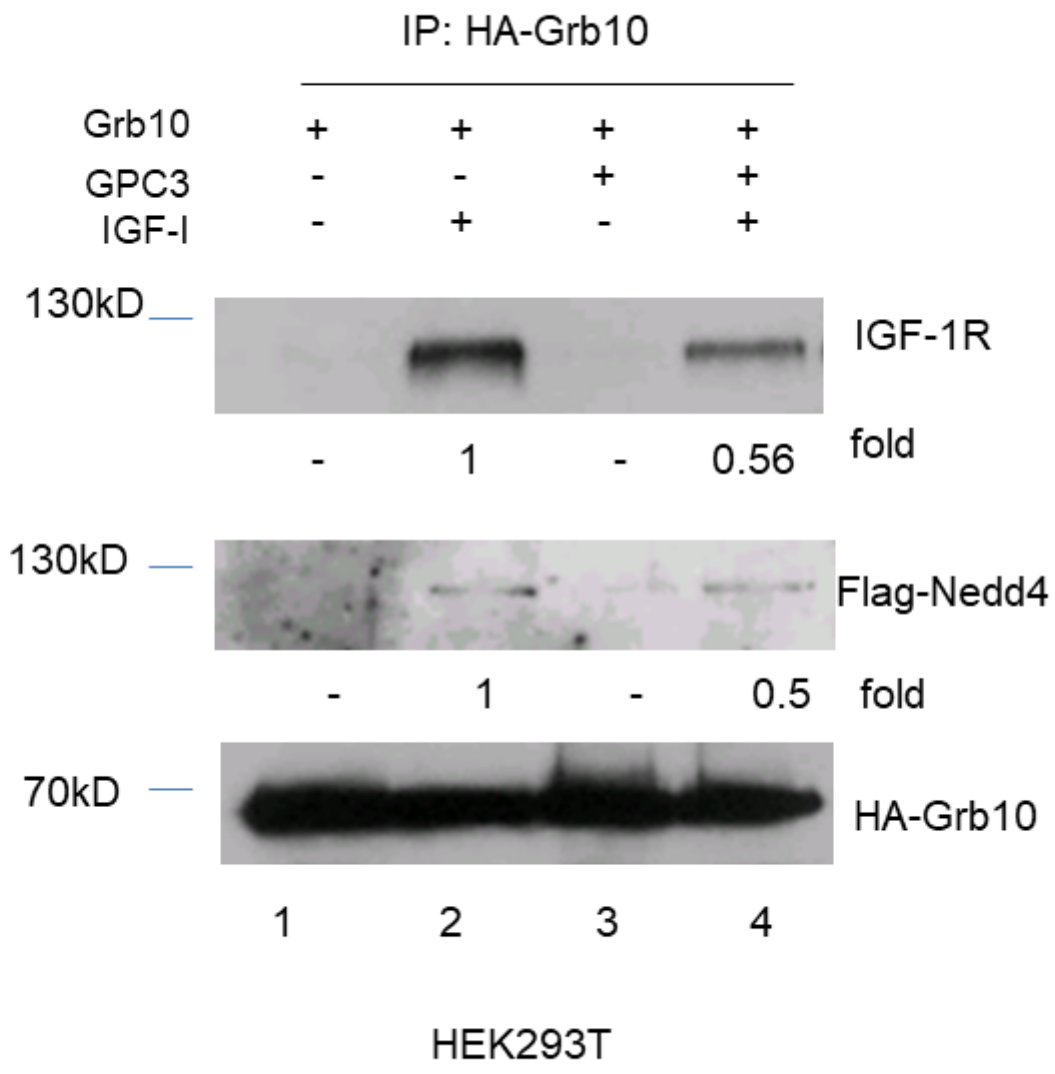

Figure 2

Less interaction between Grb10 and IGF-1R occurred in the presence of GPC3. HEK293T cells were transfected with expression vectors and stimulated with IGF-1 for 5 min. After immunoprecipitation with an anti-HA affinity matrix, IGF-1R bound to HA-Grb10 only in the presence of IGF-1 (Panel 1, lanes 2 and 4); less IGF-1R bound to HA-Grb10 in the presence of GPC3 after IGF-1 stimulation (Panel 1, lane 4). Full blots with molecular weight markers are shown in Supplementary Figure S2.

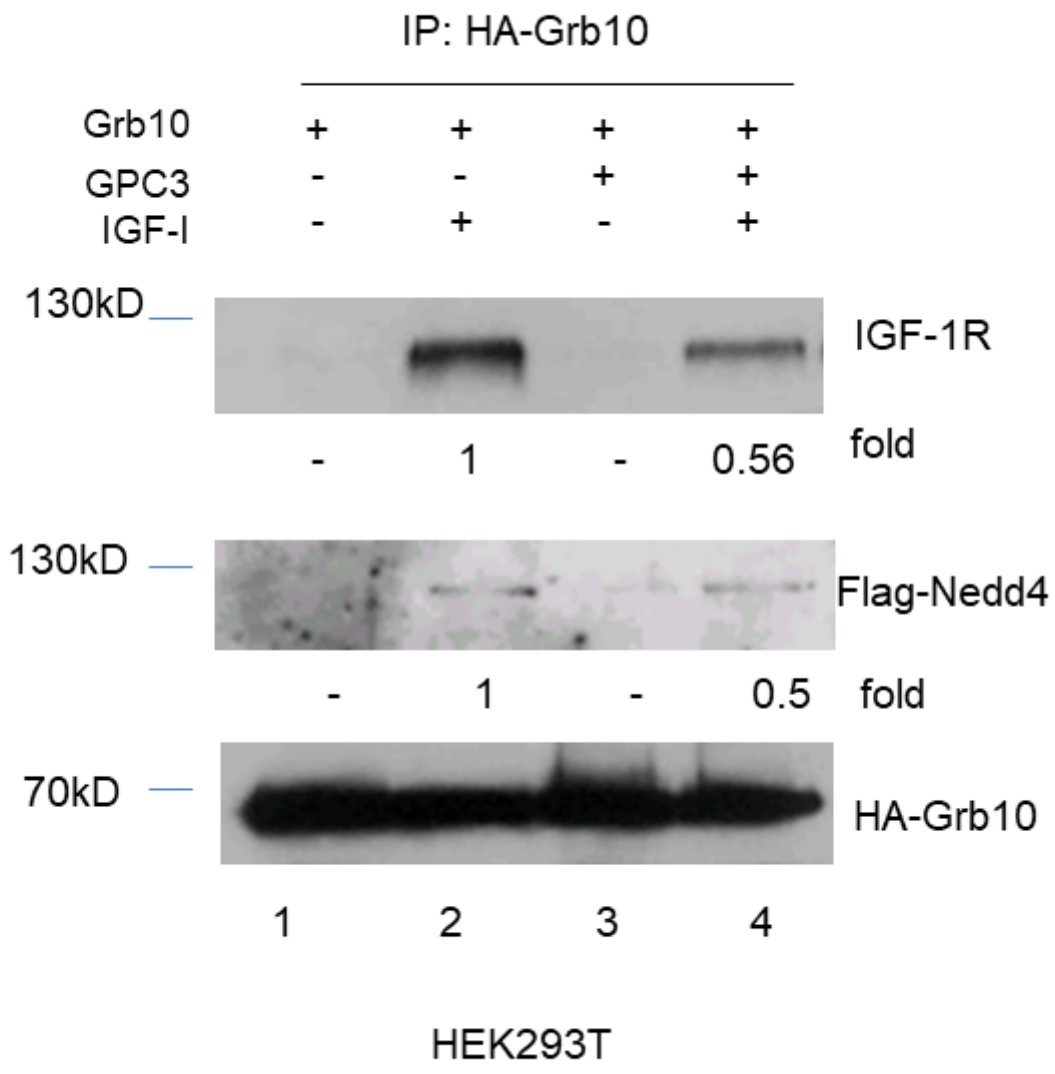

Figure 2

Less interaction between Grb10 and IGF-1R occurred in the presence of GPC3. HEK293T cells were transfected with expression vectors and stimulated with IGF-1 for 5 min. After immunoprecipitation with an anti-HA affinity matrix, IGF-1R bound to HA-Grb10 only in the presence of IGF-1 (Panel 1, lanes 2 and 4); less IGF-1R bound to HA-Grb10 in the presence of GPC3 after IGF-1 stimulation (Panel 1, lane 4). Full blots with molecular weight markers are shown in Supplementary Figure S2.

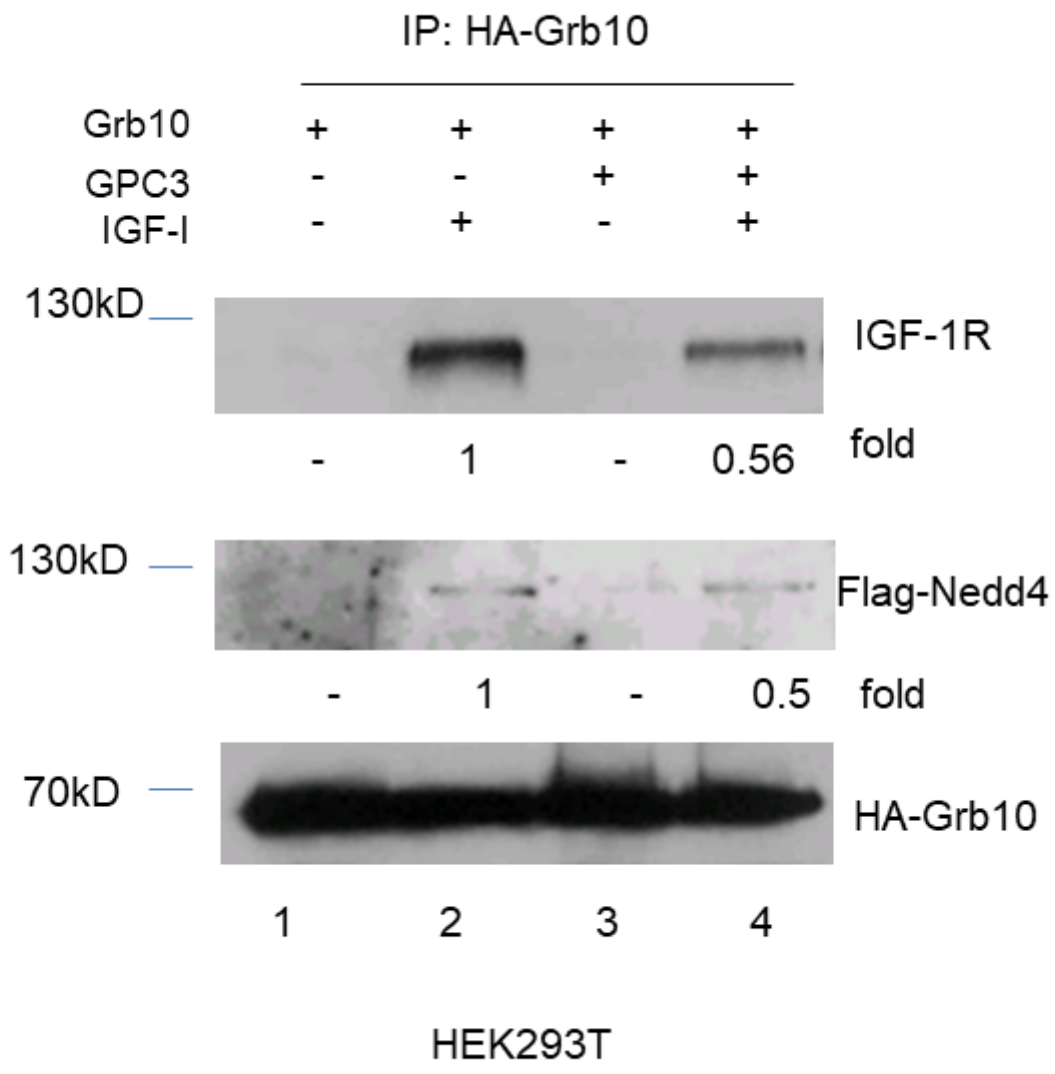

Figure 2

Less interaction between Grb10 and IGF-1R occurred in the presence of GPC3. HEK293T cells were transfected with expression vectors and stimulated with IGF-1 for 5 min. After immunoprecipitation with an anti-HA affinity matrix, IGF-1R bound to HA-Grb10 only in the presence of IGF-1 (Panel 1, lanes 2 and 4); less IGF-1R bound to HA-Grb10 in the presence of GPC3 after IGF-1 stimulation (Panel 1, lane 4). Full blots with molecular weight markers are shown in Supplementary Figure S2.

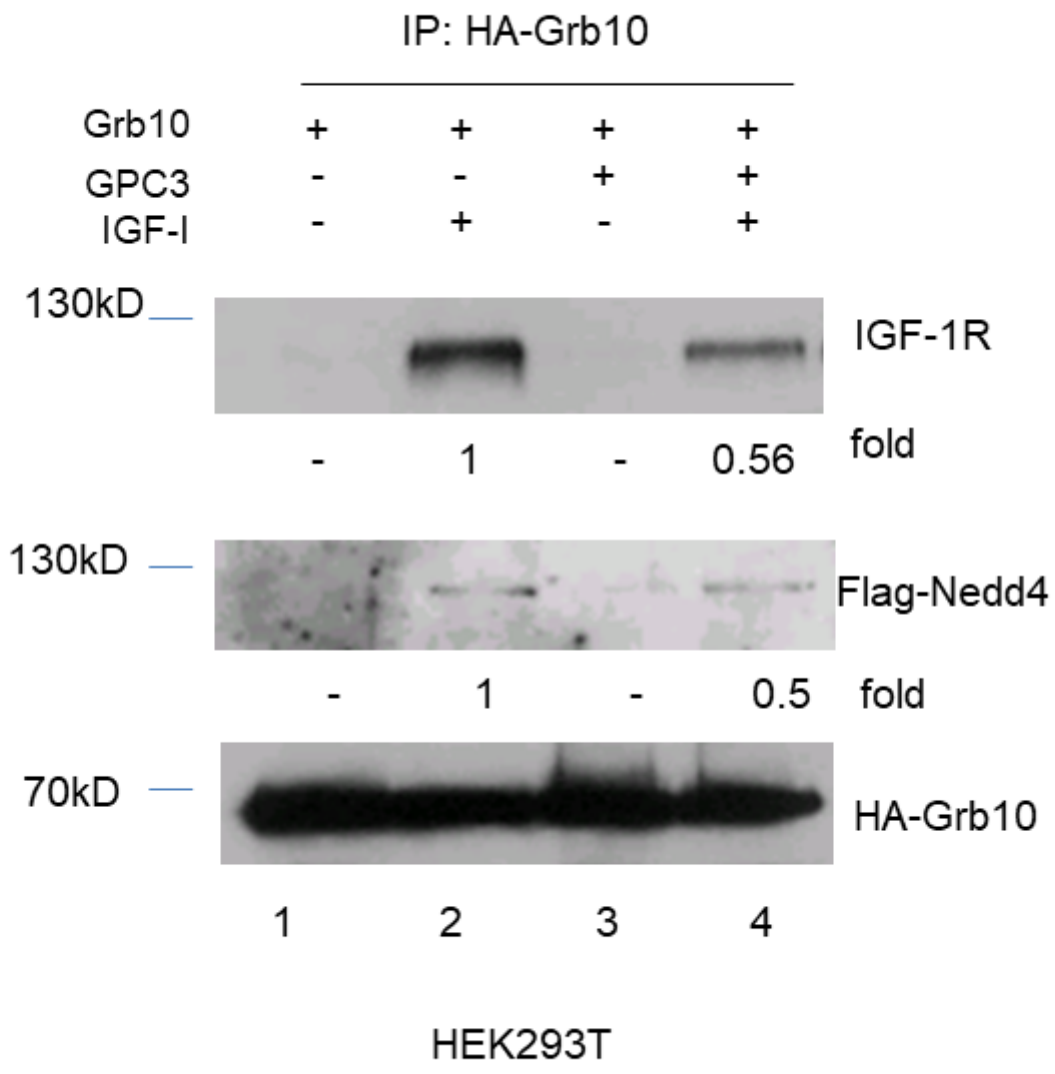

Figure 2

Less interaction between Grb10 and IGF-1R occurred in the presence of GPC3. HEK293T cells were transfected with expression vectors and stimulated with IGF-1 for 5 min. After immunoprecipitation with an anti-HA affinity matrix, IGF-1R bound to HA-Grb10 only in the presence of IGF-1 (Panel 1, lanes 2 and 4); less IGF-1R bound to HA-Grb10 in the presence of GPC3 after IGF-1 stimulation (Panel 1, lane 4). Full blots with molecular weight markers are shown in Supplementary Figure S2.

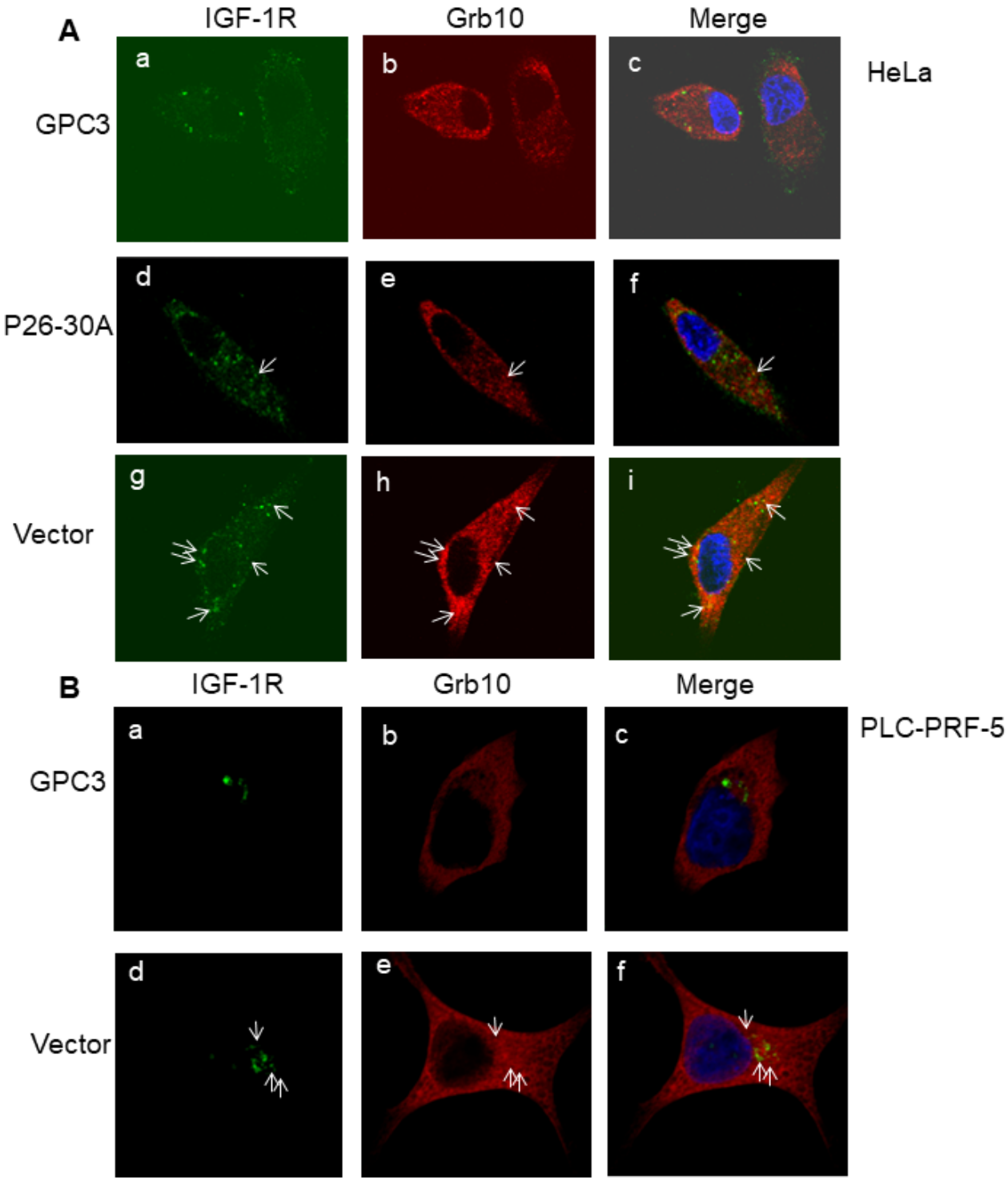

Figure 3

Less colocalization of Grb10 and IGF-1R was observed in the presence of GPC3. (A) HeLa cells were transfected with expression vectors and stimulated with IGF-1 for 10 min. Less colocalization of Grb10 and IGF-1R was found in the presence of GPC3 after IGF-1 stimulation (a–c). IGF-1R colocalized with Grb10 in the presence of P26-30A (d-f) or vector control (g–i) under IGF-1 stimulation. (B) Less colocalization of Grb10 and IGF-1R was found in the presence of GPC3 in PLC-PRF-5 cells. Stably

expressing GPC3 cells were transfected with expression vectors and stimulated with IGF-1 for 10 min. Less colocalization of Grb10 and IGF-1R was found in the presence of GPC3 after IGF-1 stimulation (a–c). IGF-1R colocalized with Grb10 (d–f) upon IGF-1 stimulation in control cells.

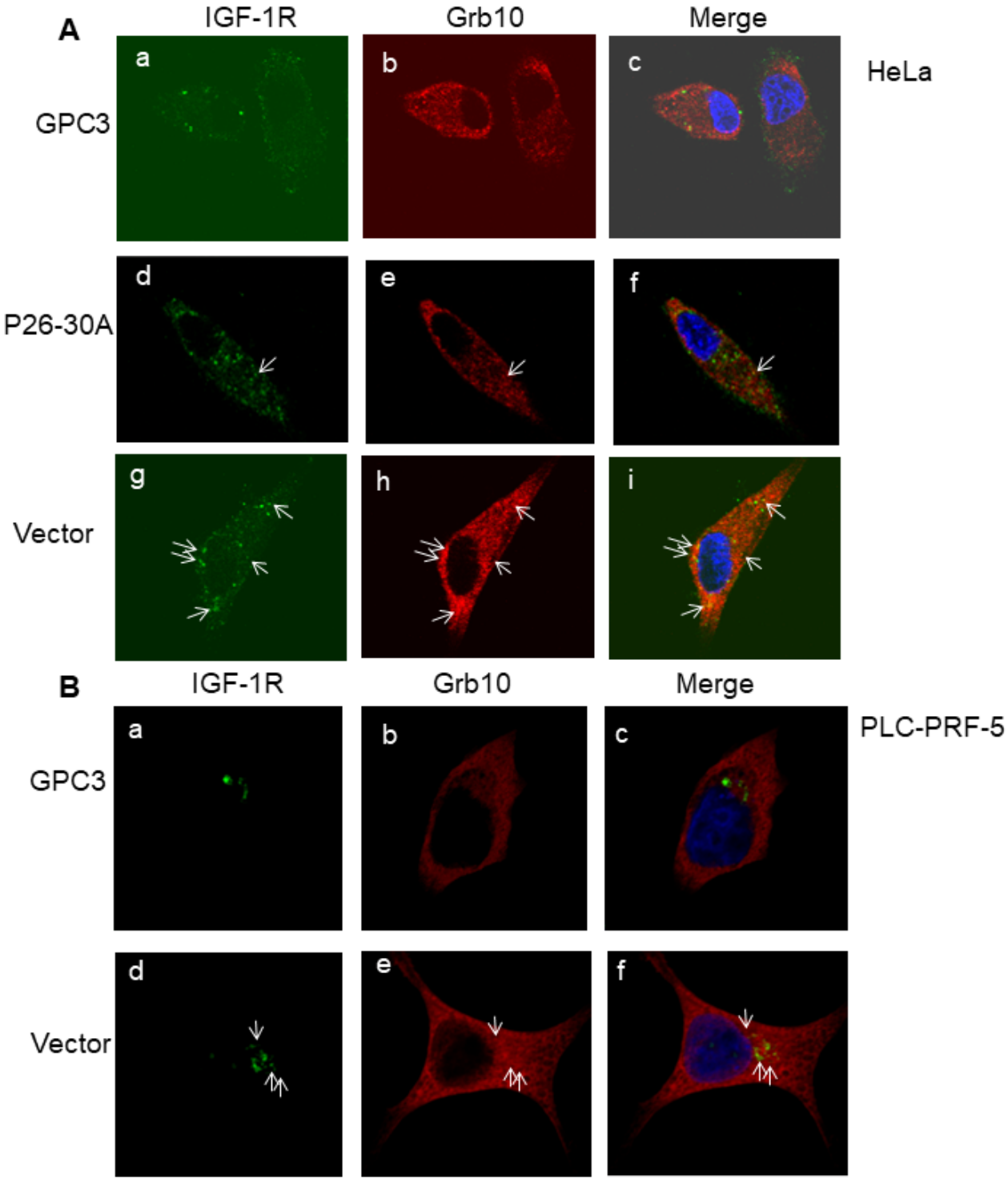

Figure 3

Less colocalization of Grb10 and IGF-1R was observed in the presence of GPC3. (A) HeLa cells were transfected with expression vectors and stimulated with IGF-1 for 10 min. Less colocalization of Grb10

and IGF-1R was found in the presence of GPC3 after IGF-1 stimulation (a–c). IGF-1R colocalized with Grb10 in the presence of P26-30A (d-f) or vector control (g–i) under IGF-1 stimulation. (B) Less colocalization of Grb10 and IGF-1R was found in the presence of GPC3 in PLC-PRF-5 cells. Stably expressing GPC3 cells were transfected with expression vectors and stimulated with IGF-1 for 10 min. Less colocalization of Grb10 and IGF-1R was found in the presence of GPC3 after IGF-1 stimulation (a–c). IGF-1R colocalized with Grb10 (d–f) upon IGF-1 stimulation in control cells.

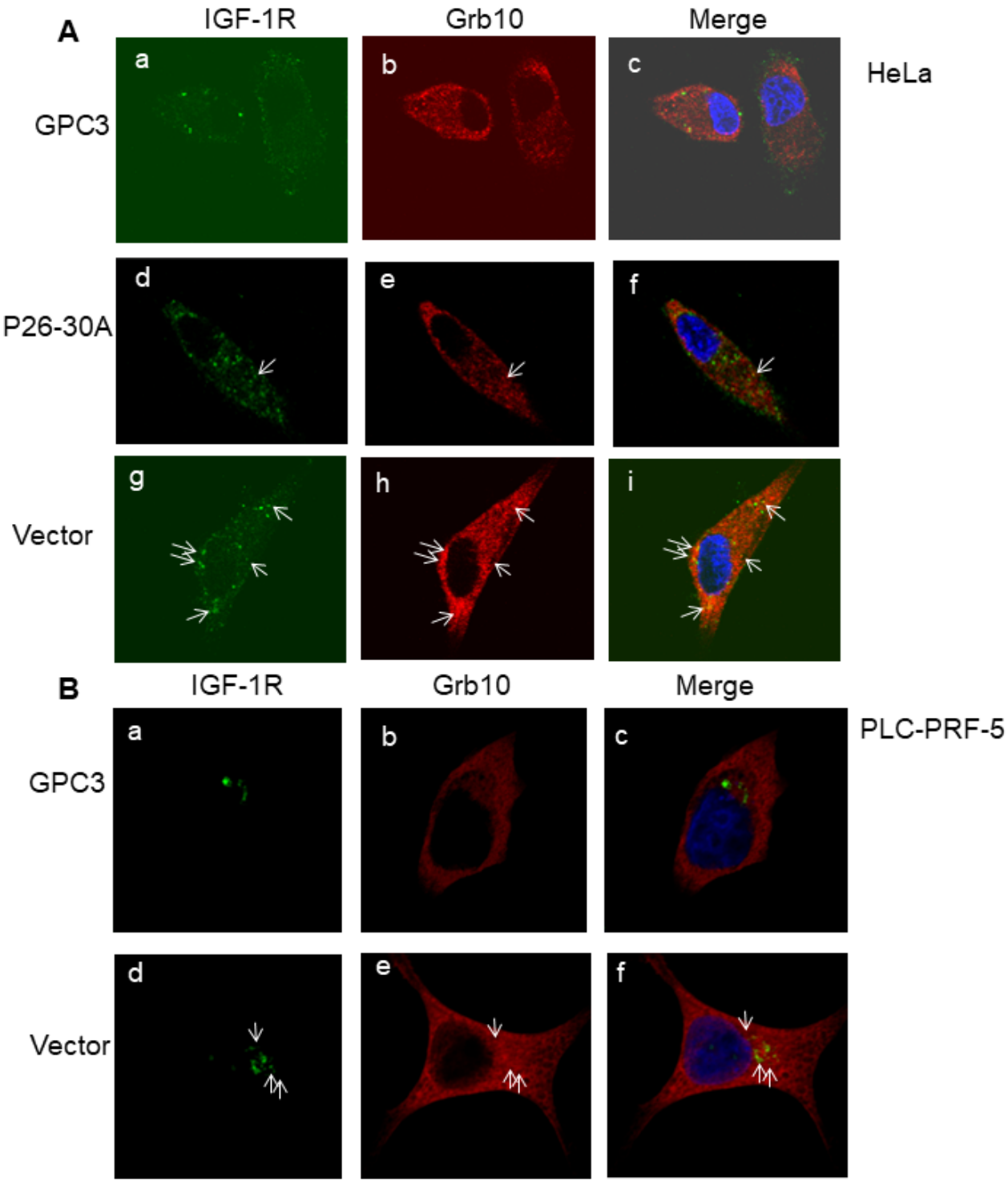

Figure 3

Less colocalization of Grb10 and IGF-1R was observed in the presence of GPC3. (A) HeLa cells were transfected with expression vectors and stimulated with IGF-1 for 10 min. Less colocalization of Grb10 and IGF-1R was found in the presence of GPC3 after IGF-1 stimulation (a–c). IGF-1R colocalized with Grb10 in the presence of P26-30A (d-f) or vector control (g–i) under IGF-1 stimulation. (B) Less colocalization of Grb10 and IGF-1R was found in the presence of GPC3 in PLC-PRF-5 cells. Stably expressing GPC3 cells were transfected with expression vectors and stimulated with IGF-1 for 10 min. Less colocalization of Grb10 and IGF-1R was found in the presence of GPC3 after IGF-1 stimulation (a–c). IGF-1R colocalized with Grb10 (d–f) upon IGF-1 stimulation in control cells.

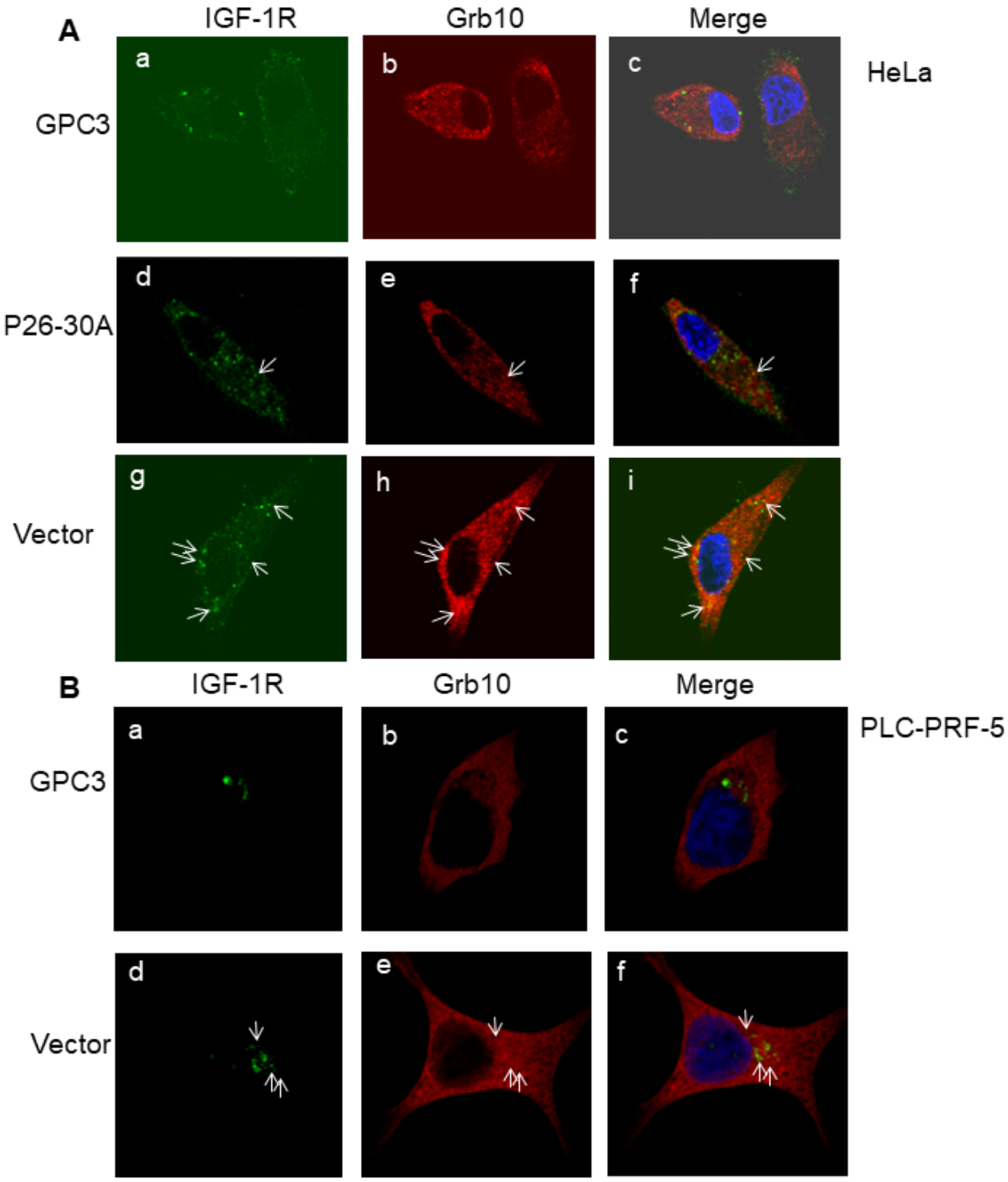

Figure 3

Less colocalization of Grb10 and IGF-1R was observed in the presence of GPC3. (A) HeLa cells were transfected with expression vectors and stimulated with IGF-1 for 10 min. Less colocalization of Grb10 and IGF-1R was found in the presence of GPC3 after IGF-1 stimulation (a–c). IGF-1R colocalized with Grb10 in the presence of P26-30A (d-f) or vector control (g–i) under IGF-1 stimulation. (B) Less colocalization of Grb10 and IGF-1R was found in the presence of GPC3 in PLC-PRF-5 cells. Stably

expressing GPC3 cells were transfected with expression vectors and stimulated with IGF-1 for 10 min. Less colocalization of Grb10 and IGF-1R was found in the presence of GPC3 after IGF-1 stimulation (a–c). IGF-1R colocalized with Grb10 (d–f) upon IGF-1 stimulation in control cells.

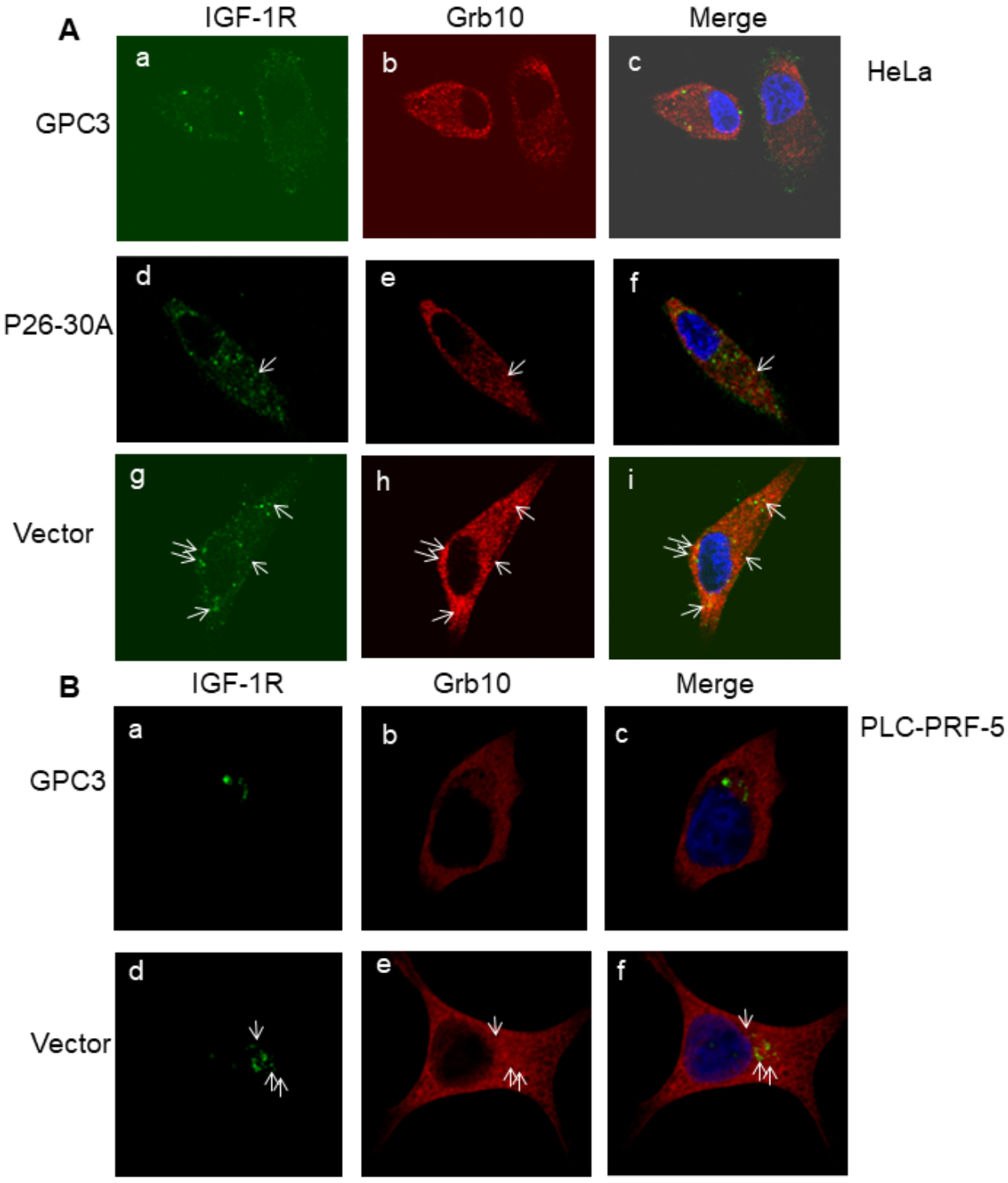

Figure 3

Less colocalization of Grb10 and IGF-1R was observed in the presence of GPC3. (A) HeLa cells were transfected with expression vectors and stimulated with IGF-1 for 10 min. Less colocalization of Grb10

and IGF-1R was found in the presence of GPC3 after IGF-1 stimulation (a–c). IGF-1R colocalized with Grb10 in the presence of P26-30A (d-f) or vector control (g–i) under IGF-1 stimulation. (B) Less colocalization of Grb10 and IGF-1R was found in the presence of GPC3 in PLC-PRF-5 cells. Stably expressing GPC3 cells were transfected with expression vectors and stimulated with IGF-1 for 10 min. Less colocalization of Grb10 and IGF-1R was found in the presence of GPC3 after IGF-1 stimulation (a–c). IGF-1R colocalized with Grb10 (d–f) upon IGF-1 stimulation in control cells.

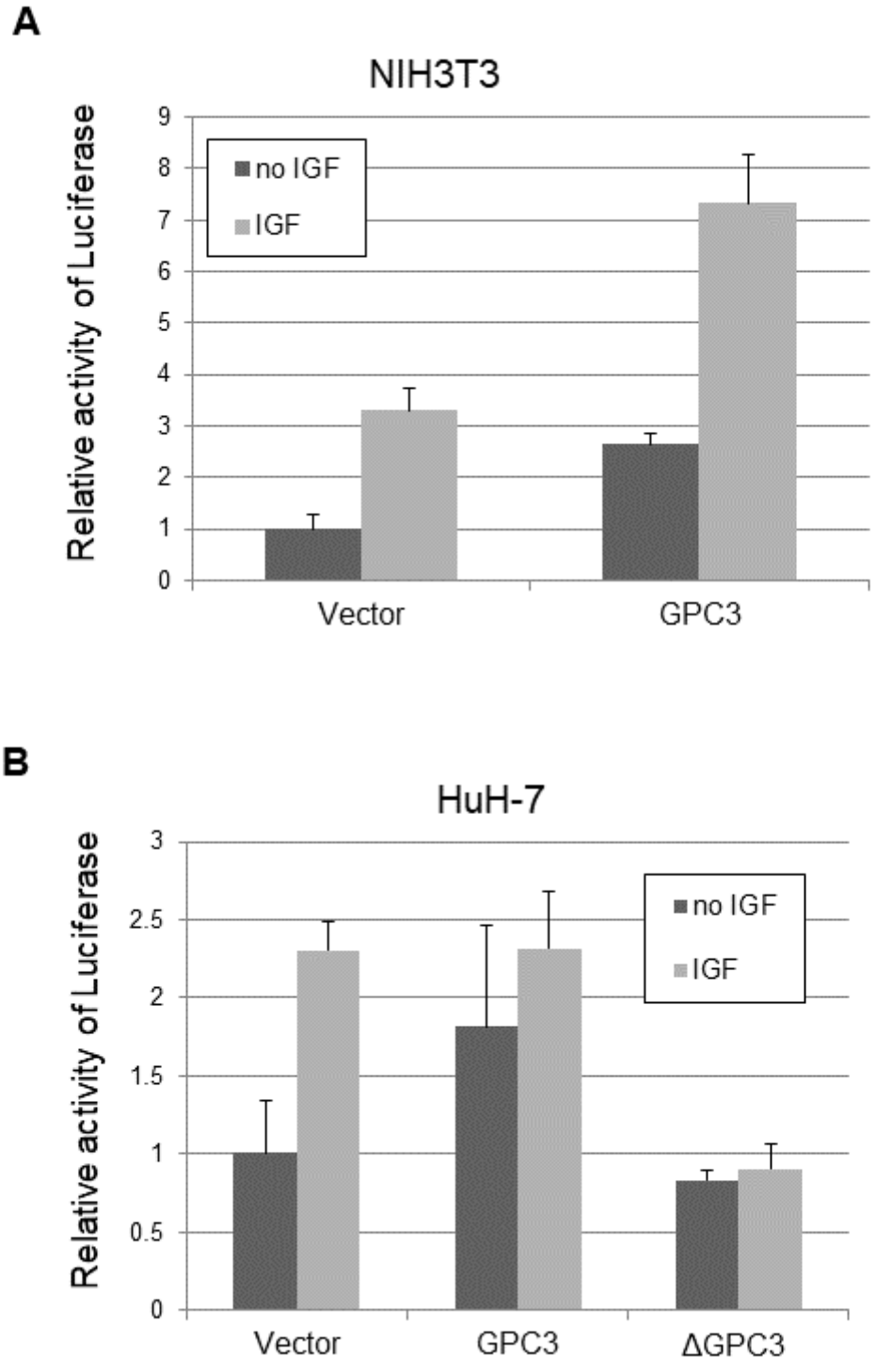

Figure 4

ΔGPC3 prevented IGF-1-stimulated AP-1 activation. (A) IGF-1 stimulated GPC3-dependent AP-1 reporter activity in NIH3T3 cells. (B) ΔGPC3 prevented IGF-1-stimulated AP-1 activation in HuH-7 cells. Cells were transfected with an empty vector, GPC3 or ΔGPC3 and were stimulated by IGF-1.

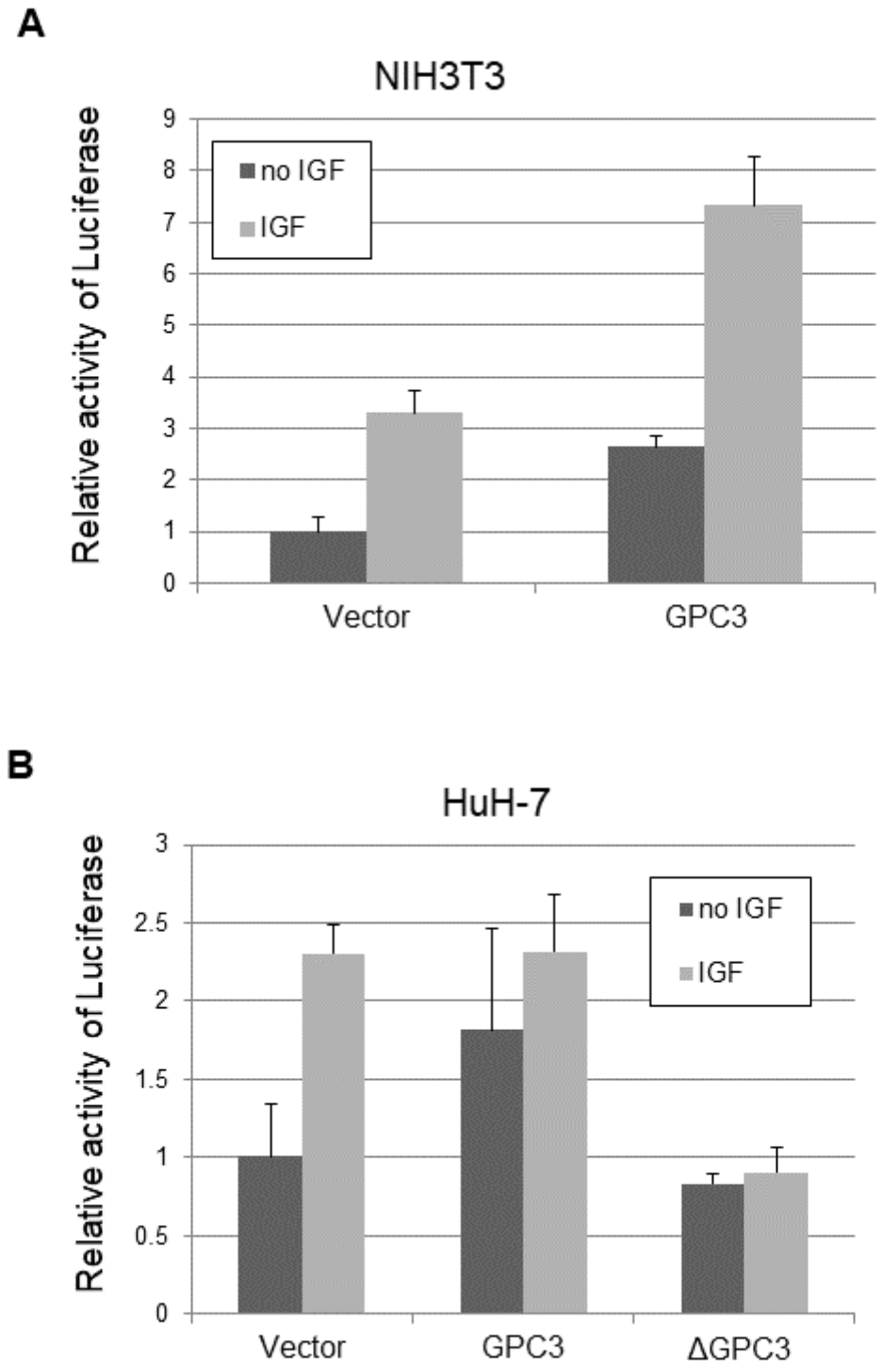

Figure 4

ΔGPC3 prevented IGF-1-stimulated AP-1 activation. (A) IGF-1 stimulated GPC3-dependent AP-1 reporter activity in NIH3T3 cells. (B) ΔGPC3 prevented IGF-1-stimulated AP-1 activation in HuH-7 cells. Cells were transfected with an empty vector, GPC3 or ΔGPC3 and were stimulated by IGF-1.

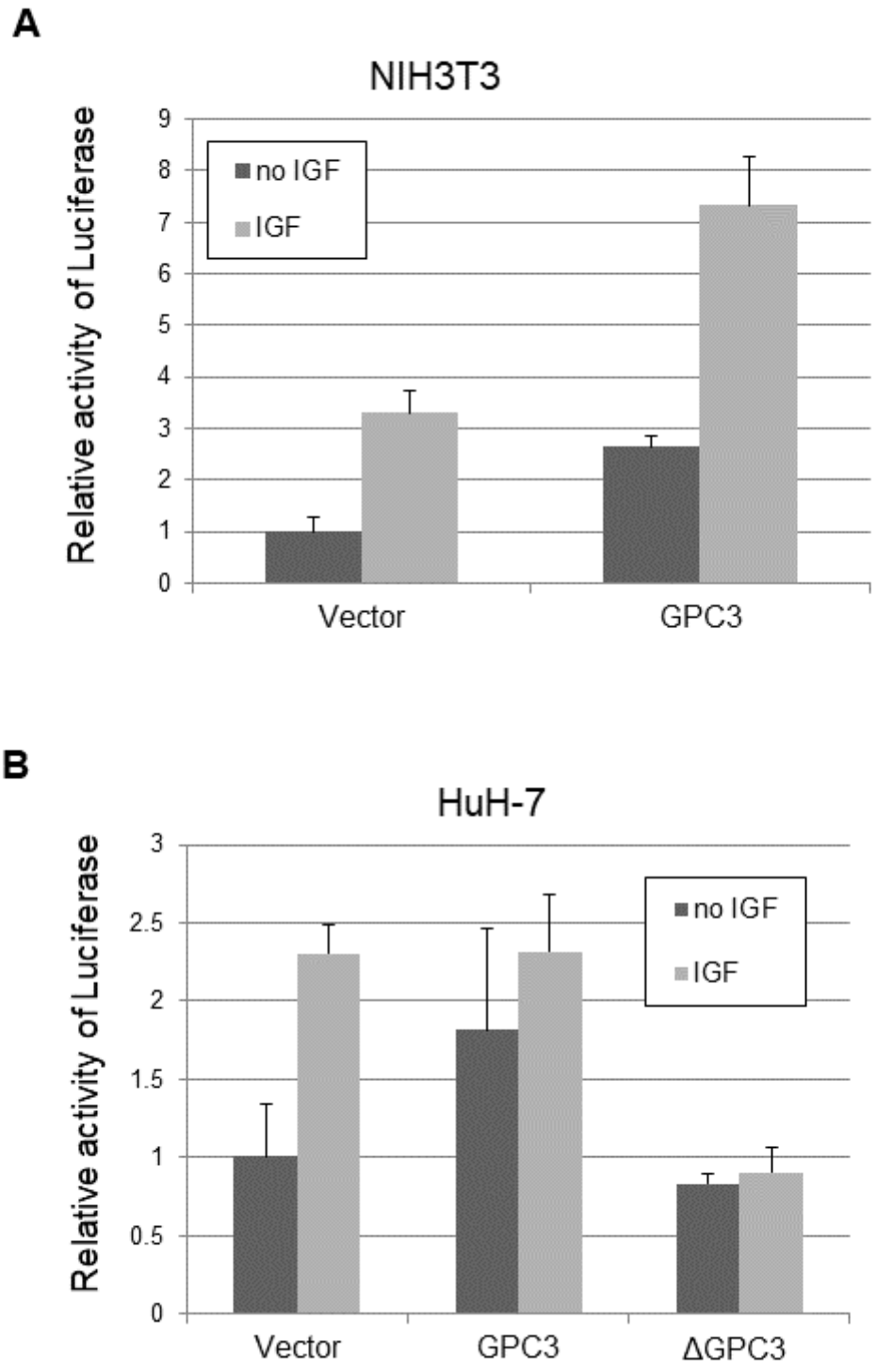

Figure 4

ΔGPC3 prevented IGF-1-stimulated AP-1 activation. (A) IGF-1 stimulated GPC3-dependent AP-1 reporter activity in NIH3T3 cells. (B) ΔGPC3 prevented IGF-1-stimulated AP-1 activation in HuH-7 cells. Cells were transfected with an empty vector, GPC3 or ΔGPC3 and were stimulated by IGF-1.

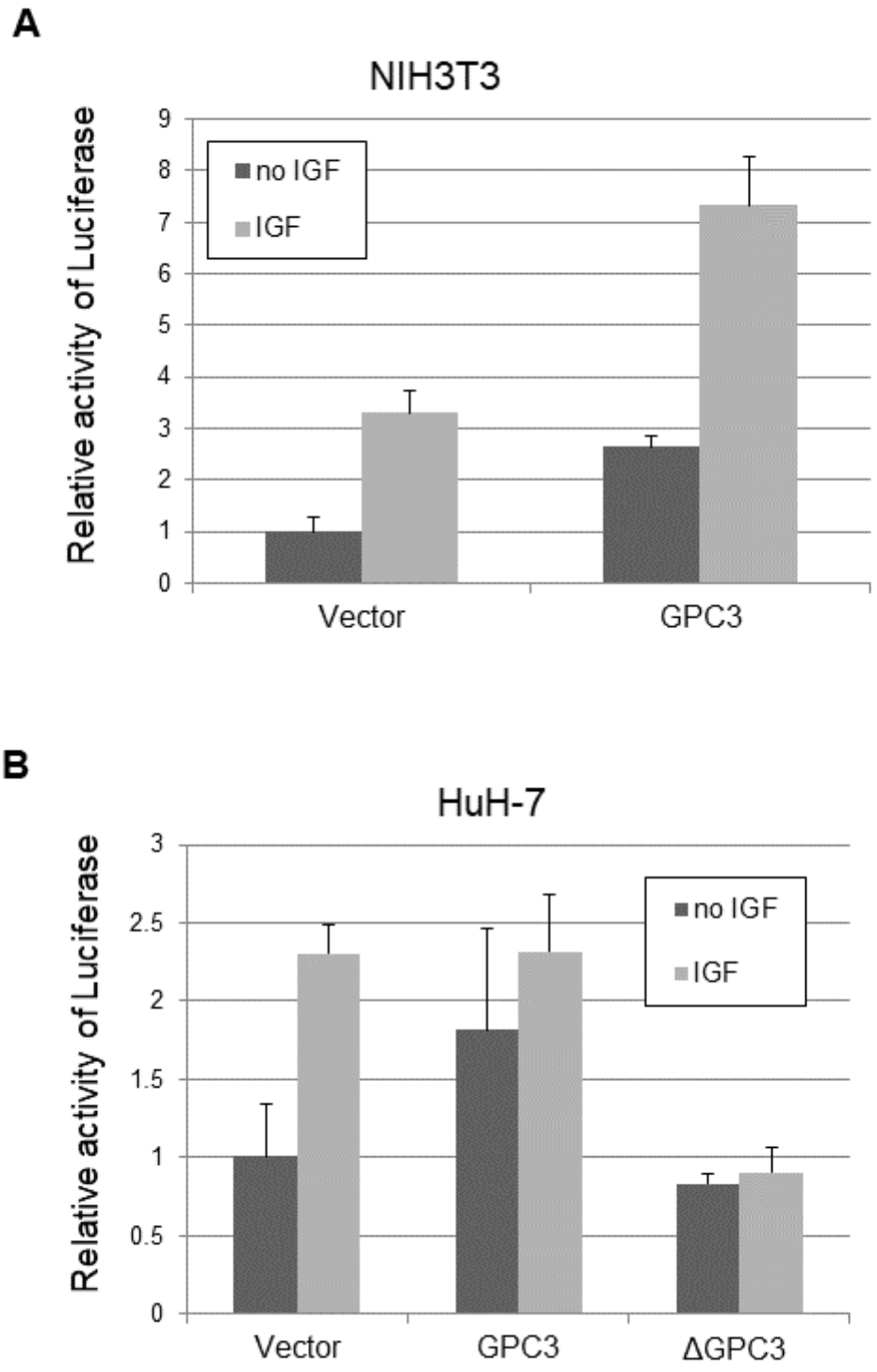

Figure 4

ΔGPC3 prevented IGF-1-stimulated AP-1 activation. (A) IGF-1 stimulated GPC3-dependent AP-1 reporter activity in NIH3T3 cells. (B) ΔGPC3 prevented IGF-1-stimulated AP-1 activation in HuH-7 cells. Cells were transfected with an empty vector, GPC3 or ΔGPC3 and were stimulated by IGF-1.

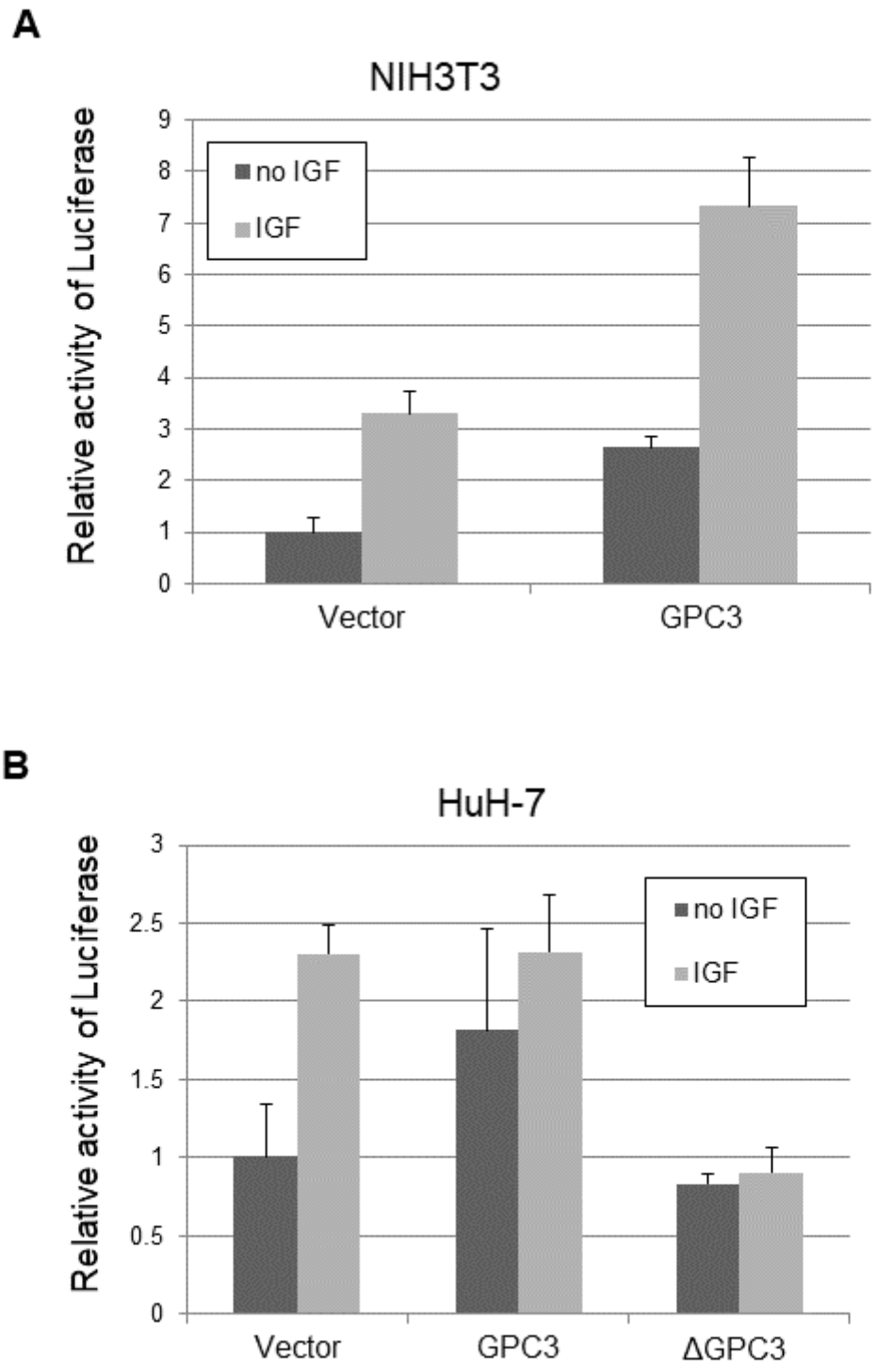

Figure 4

ΔGPC3 prevented IGF-1-stimulated AP-1 activation. (A) IGF-1 stimulated GPC3-dependent AP-1 reporter activity in NIH3T3 cells. (B) ΔGPC3 prevented IGF-1-stimulated AP-1 activation in HuH-7 cells. Cells were transfected with an empty vector, GPC3 or ΔGPC3 and were stimulated by IGF-1.

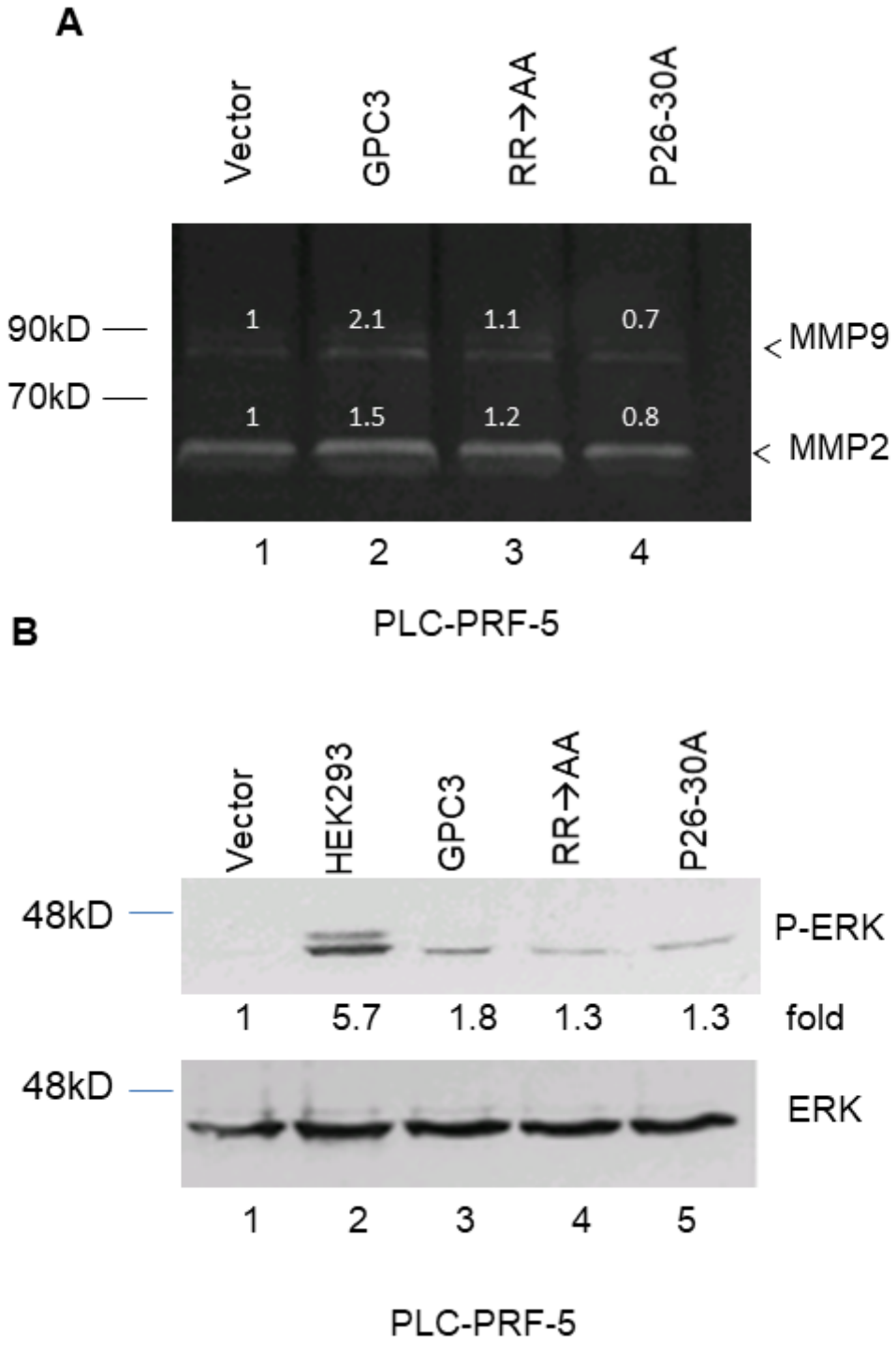

Figure 5

MMP expression and p-ERK in PLC-PRF-5 cells. (A) Quantification of MMP-2 and MMP-9 in PLC-PRF-5 conditioned medium. Cells were stably transfected with GPC3, RR→AA, P26-30A, or vector control (Vector). The conditioned medium (8 □g) of cells cultured in serum-free medium for 72 h were subjected to zymography and analyzed using densitometric analyses. Numbers above each lytic band indicate the amounts relative to the control cells. Experiments were performed in duplicate. (B) Increased p-ERK level

was observed in GPC3-expressing PLC-PRF-5 cells. Cells were serum-starved for 24 h. Cell extracts (20 µg) were immunoblotted with either antiphospho-ERK or anti-ERK. Whole cell extracts from TPA-treated HEK293 cells (lane 2) were used as a positive control. Experiments were performed in duplicate. Full blots with molecular weight markers are shown in Supplementary Figure S5B.

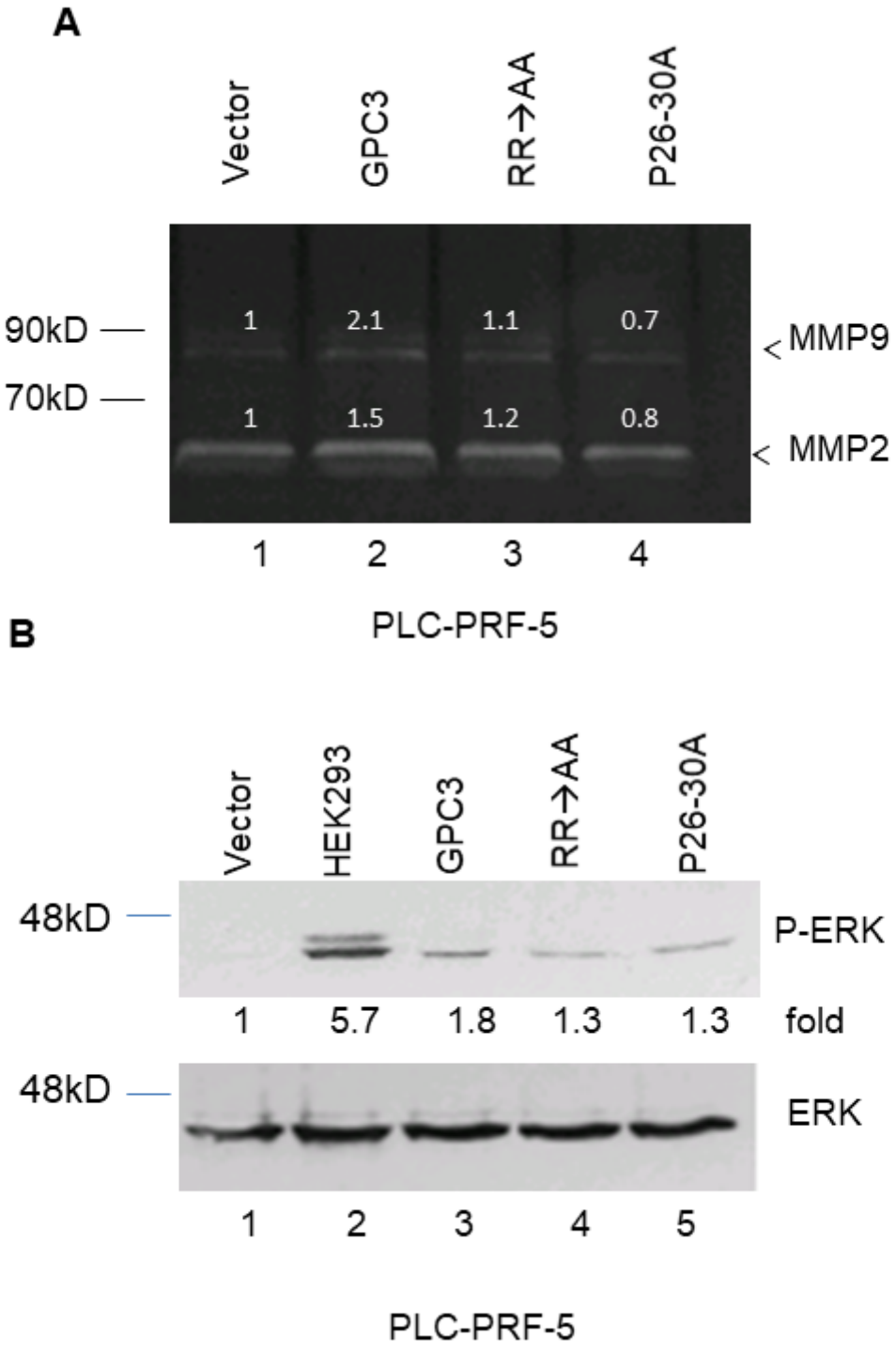

Figure 5

MMP expression and p-ERK in PLC-PRF-5 cells. (A) Quantification of MMP-2 and MMP-9 in PLC-PRF-5 conditioned medium. Cells were stably transfected with GPC3, RR→AA, P26-30A, or vector control (Vector). The conditioned medium (8 □g) of cells cultured in serum-free medium for 72 h were subjected to zymography and analyzed using densitometric analyses. Numbers above each lytic band indicate the amounts relative to the control cells. Experiments were performed in duplicate. (B) Increased p-ERK level was observed in GPC3-expressing PLC-PRF-5 cells. Cells were serum-starved for 24 h. Cell extracts (20 μg) were immunoblotted with either antiphospho-ERK or anti-ERK. Whole cell extracts from TPA-treated HEK293 cells (lane 2) were used as a positive control. Experiments were performed in duplicate. Full blots with molecular weight markers are shown in Supplementary Figure S5B.

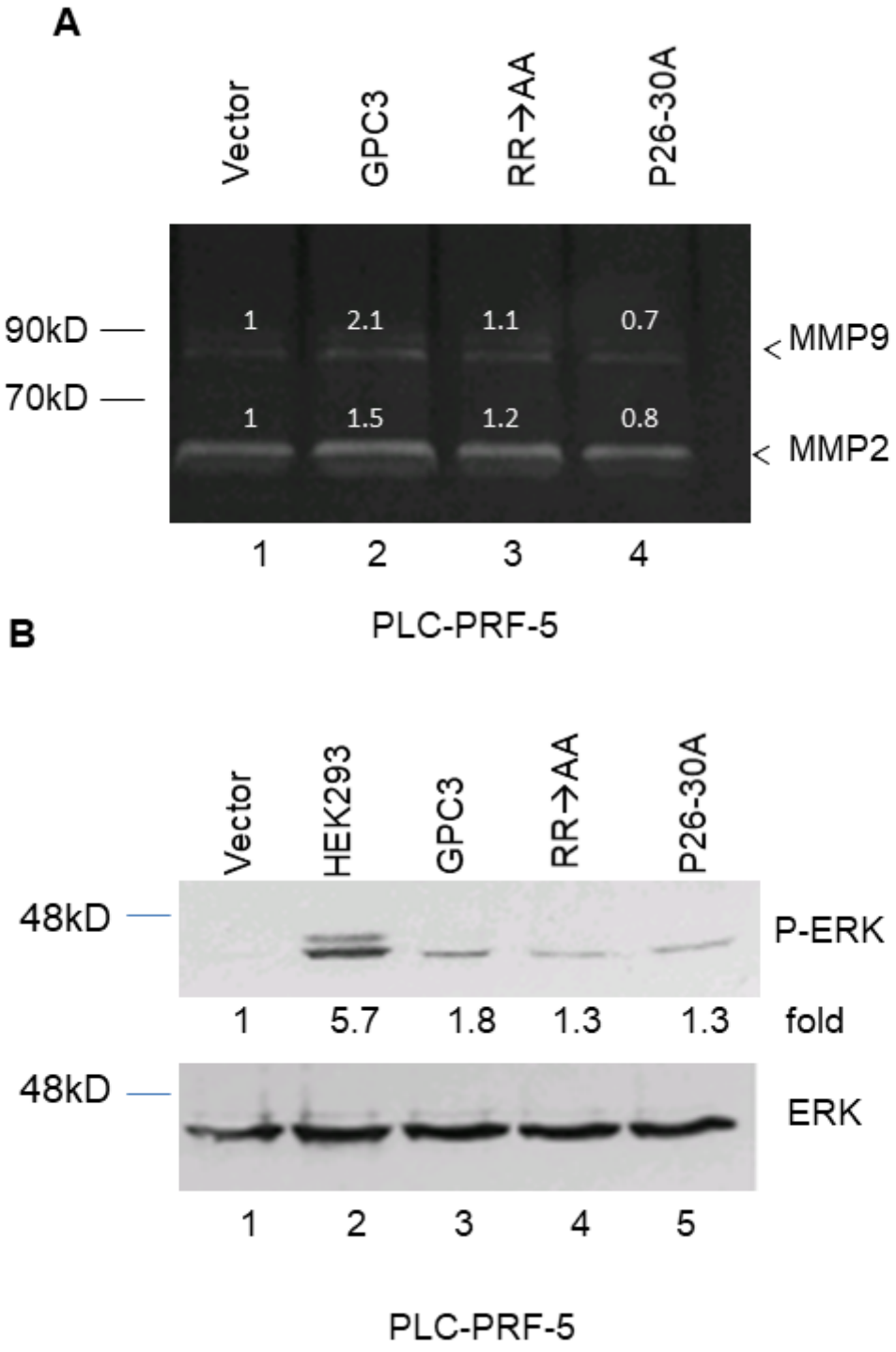

Figure 5

MMP expression and p-ERK in PLC-PRF-5 cells. (A) Quantification of MMP-2 and MMP-9 in PLC-PRF-5 conditioned medium. Cells were stably transfected with GPC3, RR→AA, P26-30A, or vector control (Vector). The conditioned medium (8 □g) of cells cultured in serum-free medium for 72 h were subjected to zymography and analyzed using densitometric analyses. Numbers above each lytic band indicate the amounts relative to the control cells. Experiments were performed in duplicate. (B) Increased p-ERK level

was observed in GPC3-expressing PLC-PRF-5 cells. Cells were serum-starved for 24 h. Cell extracts (20 µg) were immunoblotted with either antiphospho-ERK or anti-ERK. Whole cell extracts from TPA-treated HEK293 cells (lane 2) were used as a positive control. Experiments were performed in duplicate. Full blots with molecular weight markers are shown in Supplementary Figure S5B.

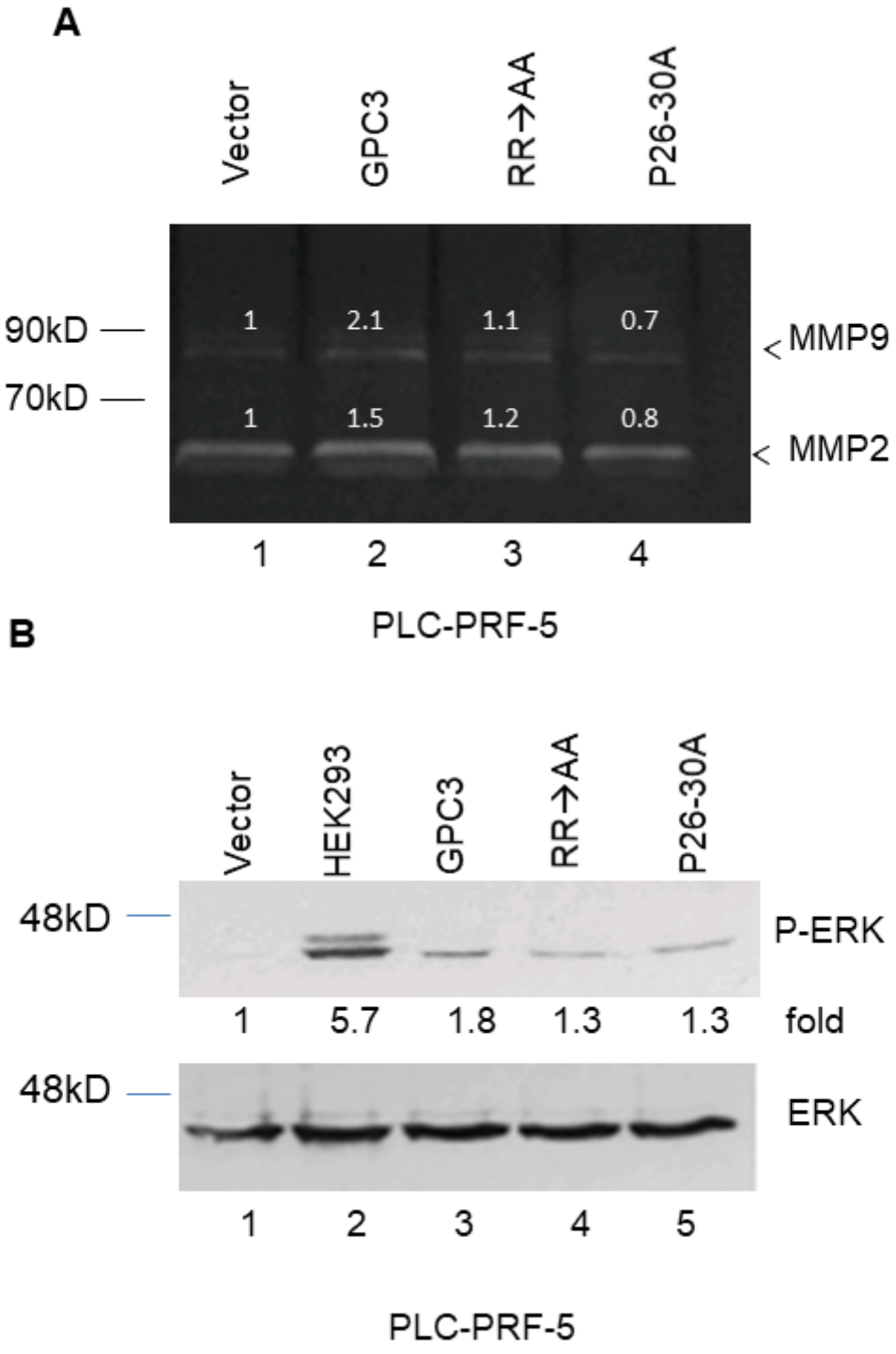

Figure 5

MMP expression and p-ERK in PLC-PRF-5 cells. (A) Quantification of MMP-2 and MMP-9 in PLC-PRF-5 conditioned medium. Cells were stably transfected with GPC3, RR→AA, P26-30A, or vector control (Vector). The conditioned medium (8 □g) of cells cultured in serum-free medium for 72 h were subjected to zymography and analyzed using densitometric analyses. Numbers above each lytic band indicate the amounts relative to the control cells. Experiments were performed in duplicate. (B) Increased p-ERK level was observed in GPC3-expressing PLC-PRF-5 cells. Cells were serum-starved for 24 h. Cell extracts (20 μg) were immunoblotted with either antiphospho-ERK or anti-ERK. Whole cell extracts from TPA-treated HEK293 cells (lane 2) were used as a positive control. Experiments were performed in duplicate. Full blots with molecular weight markers are shown in Supplementary Figure S5B.

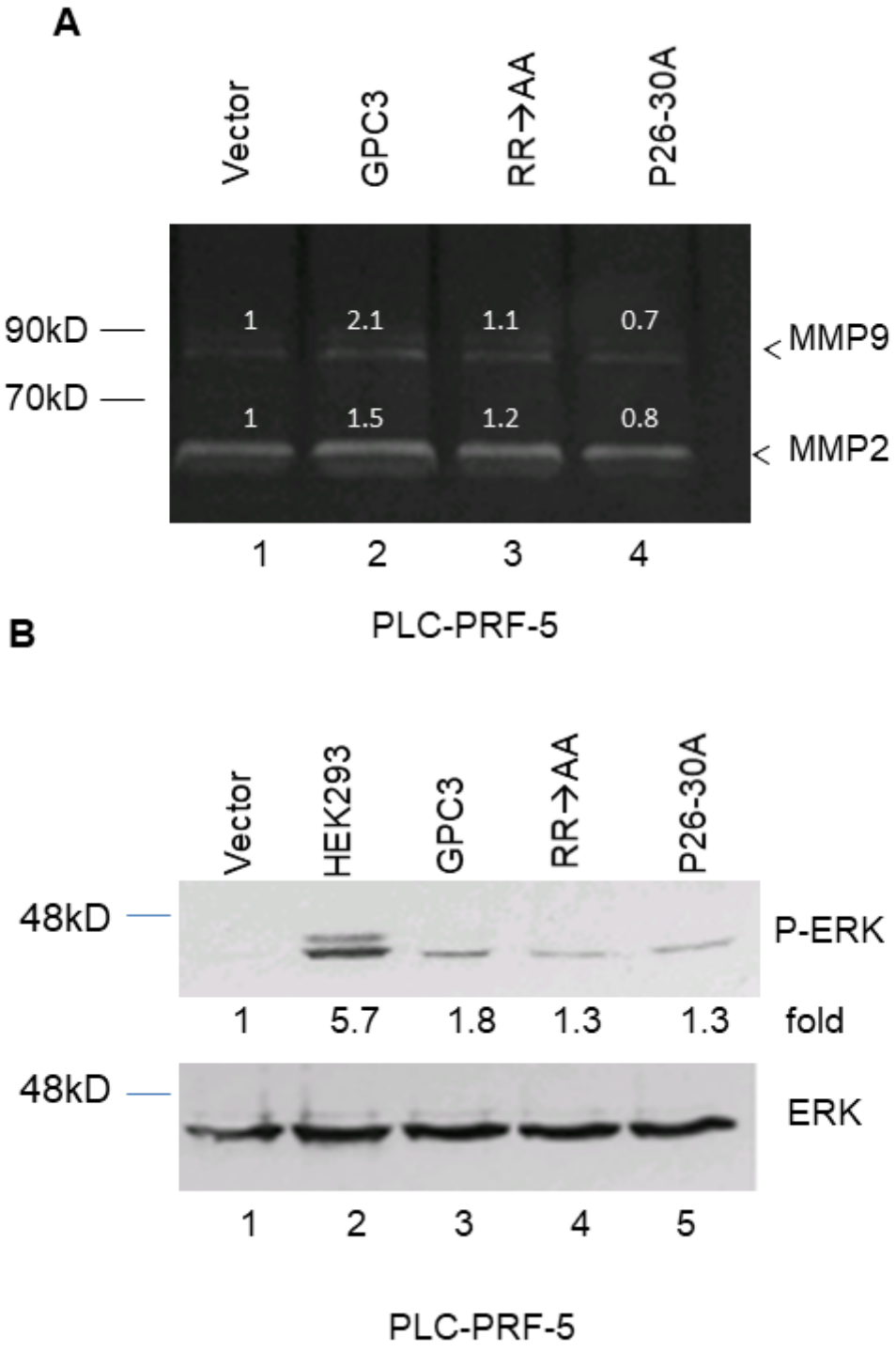

Figure 5

MMP expression and p-ERK in PLC-PRF-5 cells. (A) Quantification of MMP-2 and MMP-9 in PLC-PRF-5 conditioned medium. Cells were stably transfected with GPC3, RR→AA, P26-30A, or vector control (Vector). The conditioned medium (8 □g) of cells cultured in serum-free medium for 72 h were subjected to zymography and analyzed using densitometric analyses. Numbers above each lytic band indicate the amounts relative to the control cells. Experiments were performed in duplicate. (B) Increased p-ERK level

was observed in GPC3-expressing PLC-PRF-5 cells. Cells were serum-starved for 24 h. Cell extracts (20 µg) were immunoblotted with either antiphospho-ERK or anti-ERK. Whole cell extracts from TPA-treated HEK293 cells (lane 2) were used as a positive control. Experiments were performed in duplicate. Full blots with molecular weight markers are shown in Supplementary Figure S5B.

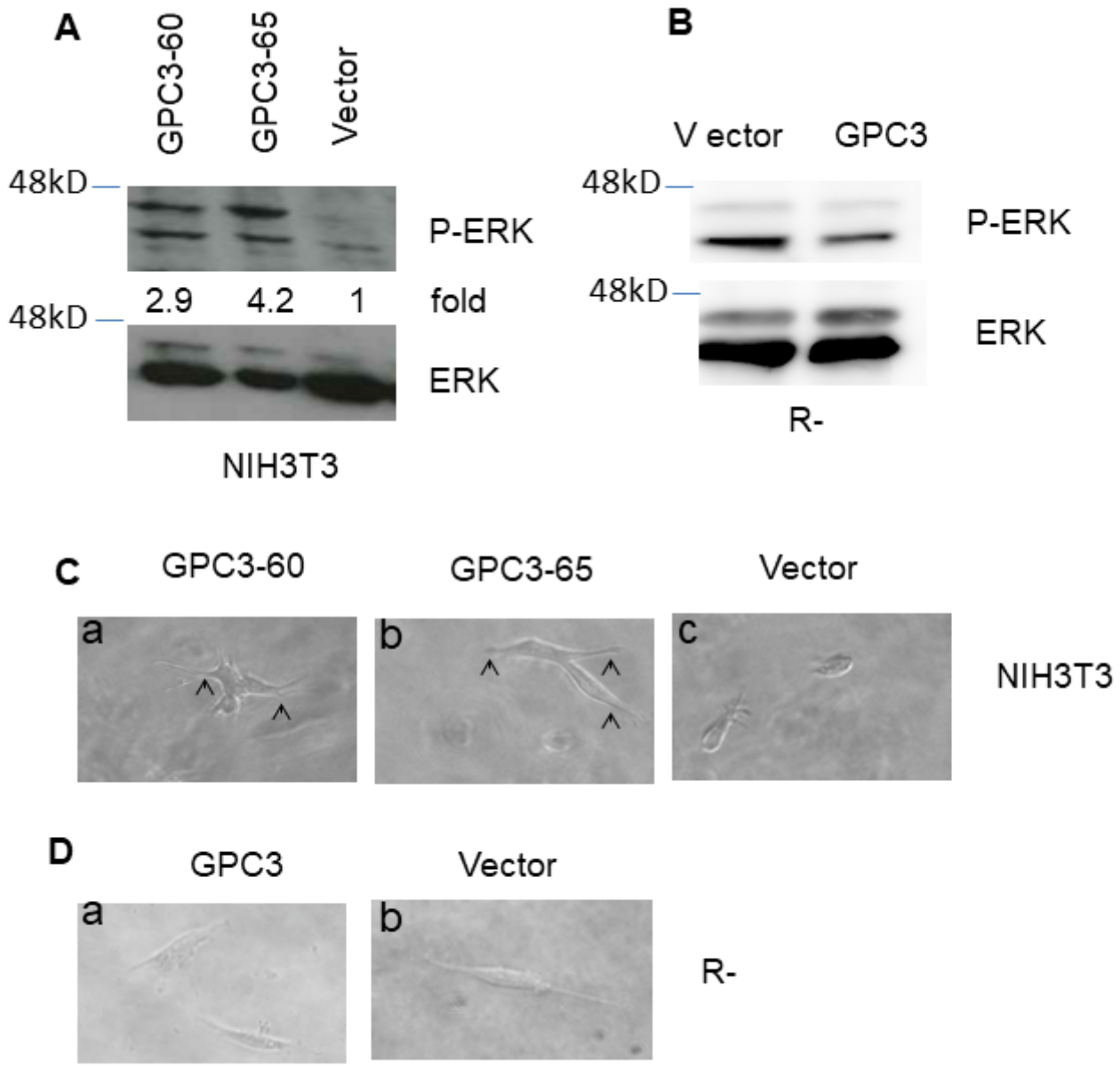

Figure 6

Expression of p-ERK and invasion in GPC3-expressing cells. (A) Expression of p-ERK was higher in GPC3-expressing NIH3T3 cells. Cells were serum-starved for 24 h. Cell extracts (15 µg) were immunoblotted with either antiphospho-ERK or anti-ERK. Full blots with molecular weight markers are shown in Supplementary Figure S6A. (B) p-ERK was not activated in GPC3-expressing R-cells. Cells were serum-starved for 24 h. Cell extracts (30 µg) were immunoblotted with either antiphospho-ERK or anti-ERK. Full blots with molecular weight markers are shown in Supplementary Figure S6B. (C) NIH3T3 cells grown in

3D collagen I gels. Morphology of GPC3-60 (a), GPC3-65 (b) or vector control (c) cells embedded in collagen I gels (final collagen I concentration of 2.3 mg/ml). Arrowheads indicate invasively growing tips. (D) R-cells grown in 3D collagen I gels. Morphology of GPC3 (a) or vector control (b) cells embedded in collagen I gels (final collagen I concentration of 2.3 mg/ml).

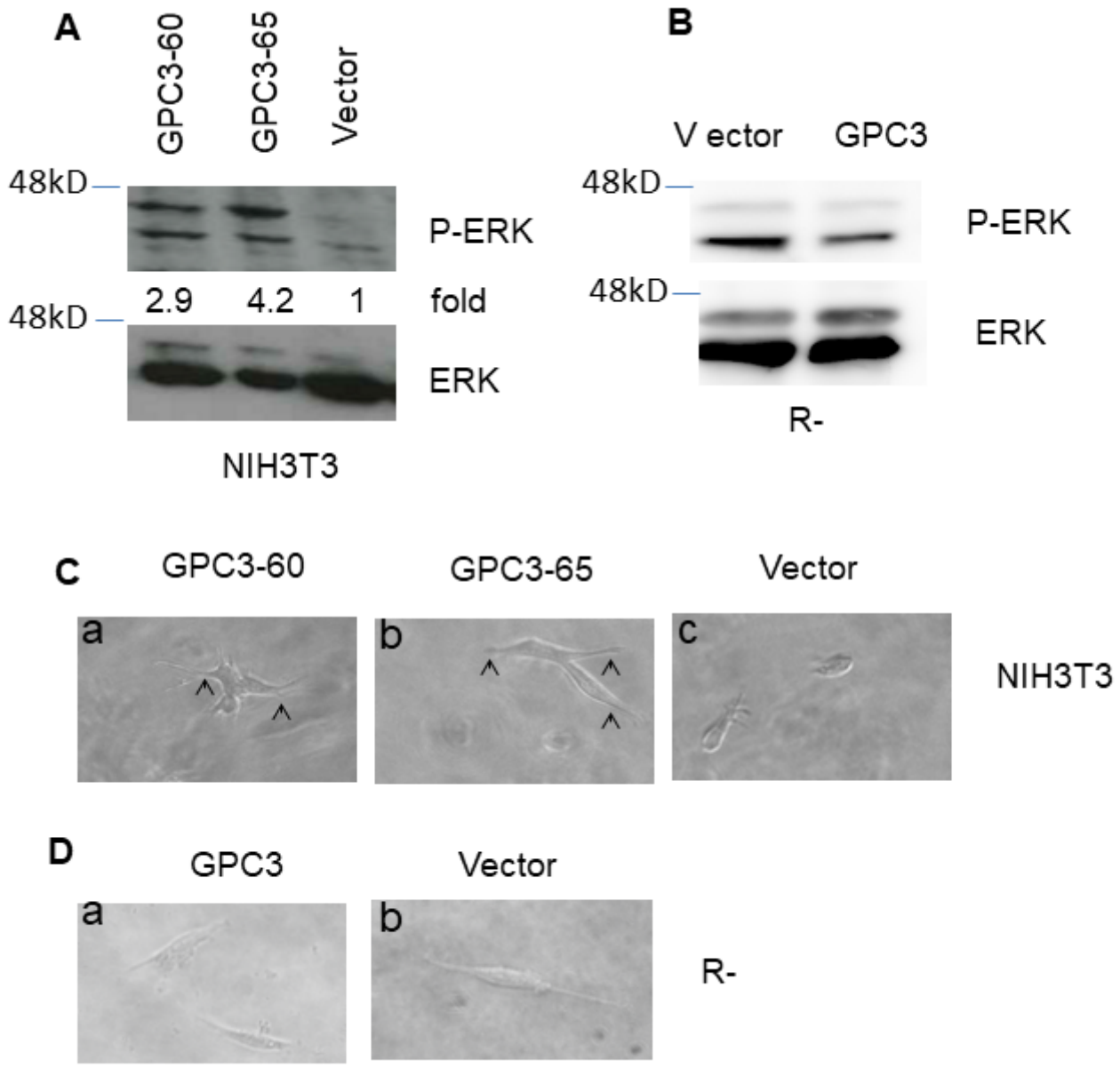

Figure 6

Expression of p-ERK and invasion in GPC3-expressing cells. (A) Expression of p-ERK was higher in GPC3-expressing NIH3T3 cells. Cells were serum-starved for 24 h. Cell extracts (15 µg) were immunoblotted with either antiphospho-ERK or anti-ERK. Full blots with molecular weight markers are shown in Supplementary Figure S6A. (B) p-ERK was not activated in GPC3-expressing R-cells. Cells were serum-starved for 24 h. Cell extracts (30 µg) were immunoblotted with either antiphospho-ERK or anti-ERK. Full blots with molecular weight markers are shown in Supplementary Figure S6B. (C) NIH3T3 cells grown in

3D collagen I gels. Morphology of GPC3-60 (a), GPC3-65 (b) or vector control (c) cells embedded in collagen I gels (final collagen I concentration of 2.3 mg/ml). Arrowheads indicate invasively growing tips. (D) R-cells grown in 3D collagen I gels. Morphology of GPC3 (a) or vector control (b) cells embedded in collagen I gels (final collagen I concentration of 2.3 mg/ml).

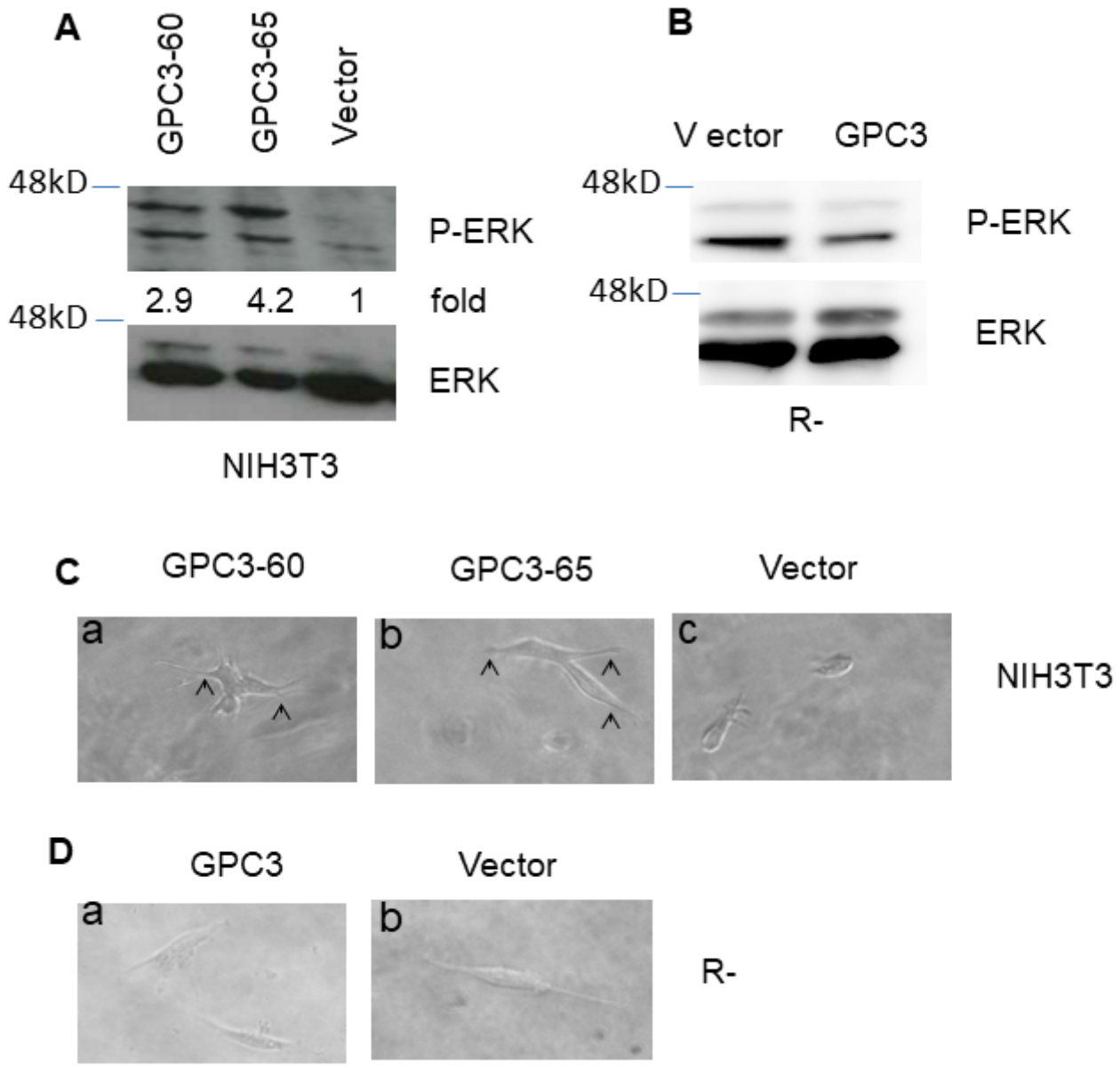

Figure 6

Expression of p-ERK and invasion in GPC3-expressing cells. (A) Expression of p-ERK was higher in GPC3-expressing NIH3T3 cells. Cells were serum-starved for 24 h. Cell extracts (15 µg) were immunoblotted with either antiphospho-ERK or anti-ERK. Full blots with molecular weight markers are shown in Supplementary Figure S6A. (B) p-ERK was not activated in GPC3-expressing R-cells. Cells were serum-starved for 24 h. Cell extracts (30 µg) were immunoblotted with either antiphospho-ERK or anti-ERK. Full blots with molecular weight markers are shown in Supplementary Figure S6B. (C) NIH3T3 cells grown in

3D collagen I gels. Morphology of GPC3-60 (a), GPC3-65 (b) or vector control (c) cells embedded in collagen I gels (final collagen I concentration of 2.3 mg/ml). Arrowheads indicate invasively growing tips. (D) R-cells grown in 3D collagen I gels. Morphology of GPC3 (a) or vector control (b) cells embedded in collagen I gels (final collagen I concentration of 2.3 mg/ml).

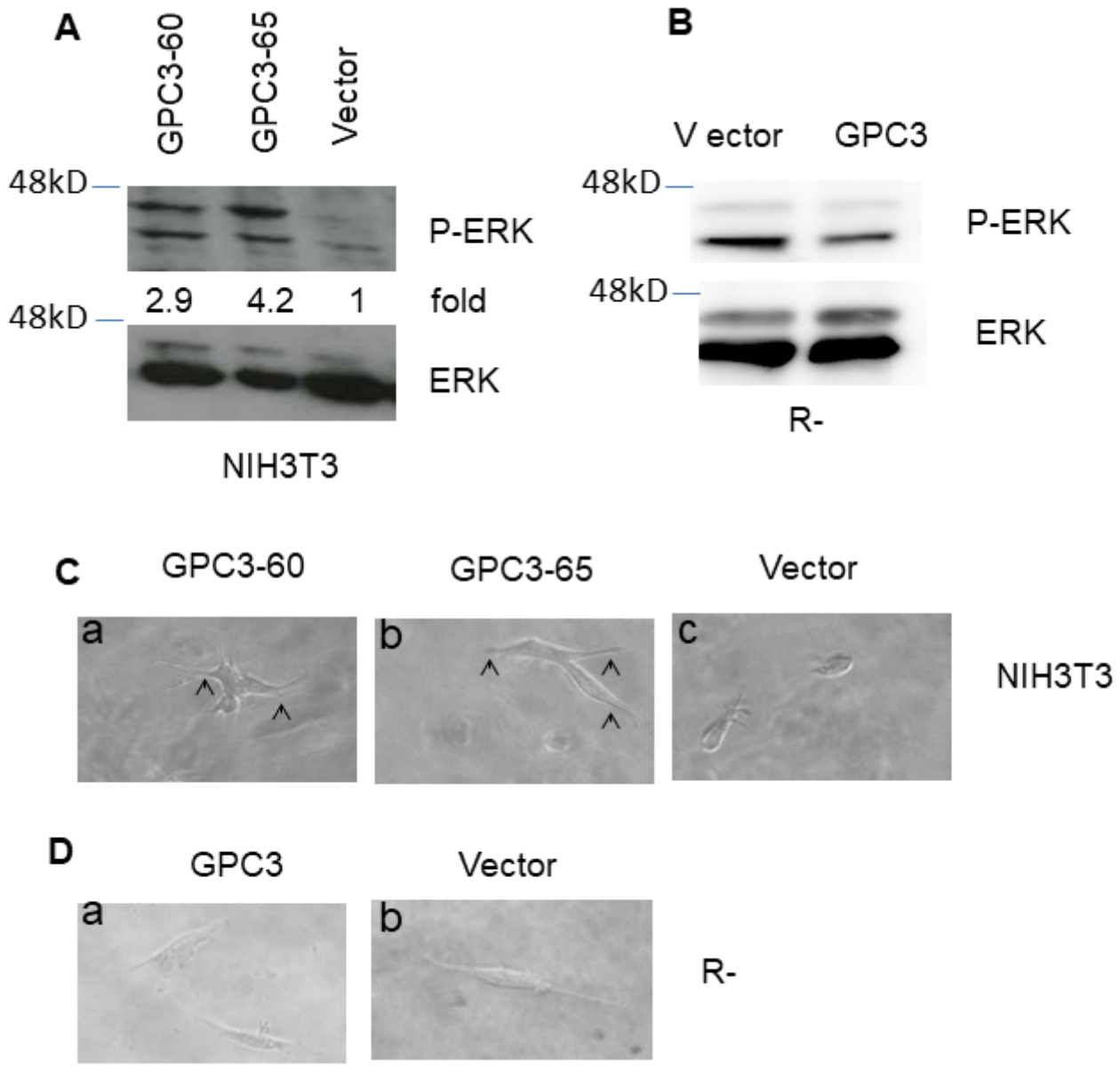

Figure 6

Expression of p-ERK and invasion in GPC3-expressing cells. (A) Expression of p-ERK was higher in GPC3-expressing NIH3T3 cells. Cells were serum-starved for 24 h. Cell extracts (15 µg) were immunoblotted with either antiphospho-ERK or anti-ERK. Full blots with molecular weight markers are shown in Supplementary Figure S6A. (B) p-ERK was not activated in GPC3-expressing R-cells. Cells were serum-starved for 24 h. Cell extracts (30 µg) were immunoblotted with either antiphospho-ERK or anti-ERK. Full blots with molecular weight markers are shown in Supplementary Figure S6B. (C) NIH3T3 cells grown in

3D collagen I gels. Morphology of GPC3-60 (a), GPC3-65 (b) or vector control (c) cells embedded in collagen I gels (final collagen I concentration of 2.3 mg/ml). Arrowheads indicate invasively growing tips. (D) R-cells grown in 3D collagen I gels. Morphology of GPC3 (a) or vector control (b) cells embedded in collagen I gels (final collagen I concentration of 2.3 mg/ml).

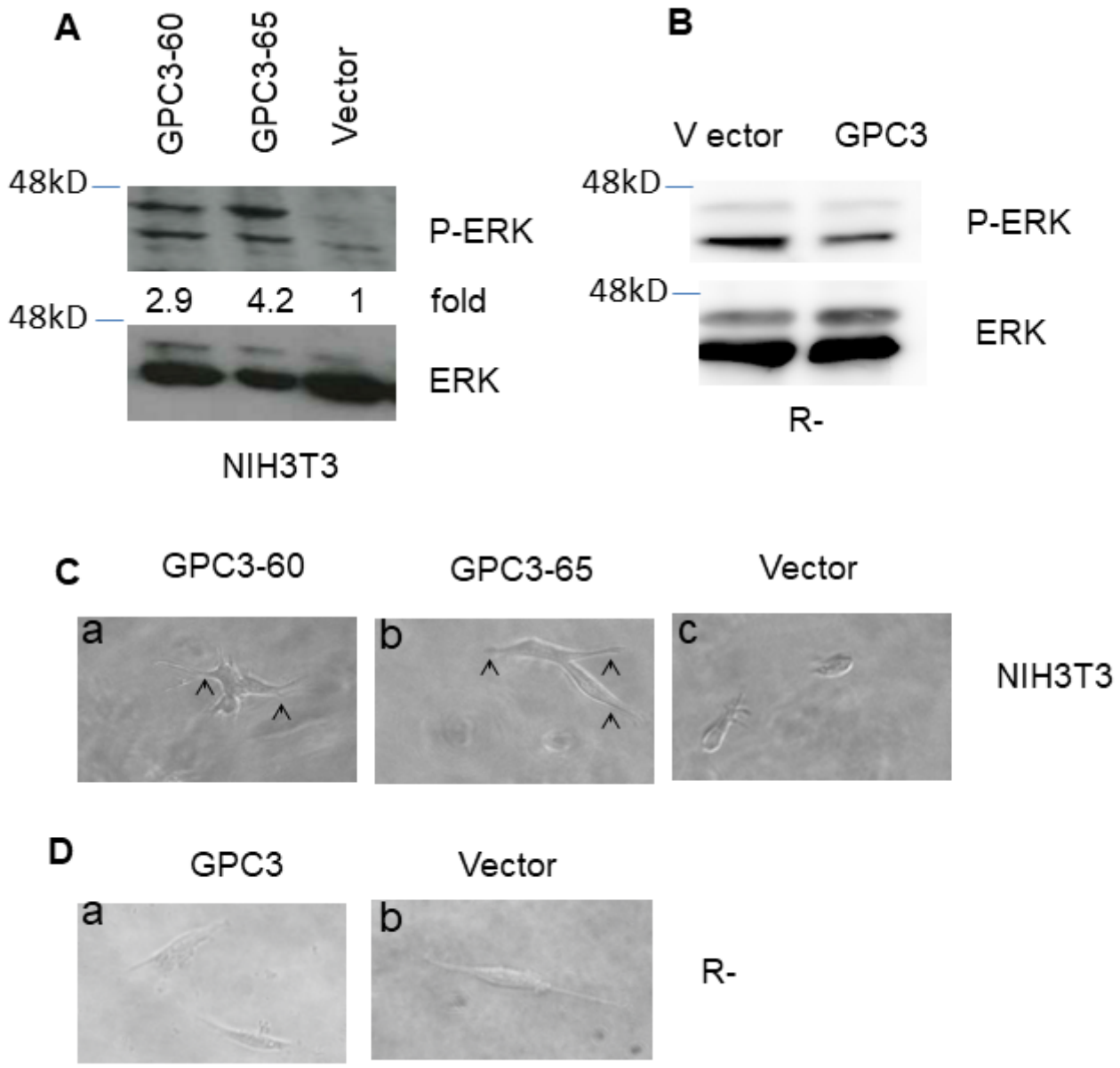

Figure 6

Expression of p-ERK and invasion in GPC3-expressing cells. (A) Expression of p-ERK was higher in GPC3-expressing NIH3T3 cells. Cells were serum-starved for 24 h. Cell extracts (15 µg) were immunoblotted with either antiphospho-ERK or anti-ERK. Full blots with molecular weight markers are shown in Supplementary Figure S6A. (B) p-ERK was not activated in GPC3-expressing R-cells. Cells were serum-starved for 24 h. Cell extracts (30 µg) were immunoblotted with either antiphospho-ERK or anti-ERK. Full blots with molecular weight markers are shown in Supplementary Figure S6B. (C) NIH3T3 cells grown in

3D collagen I gels. Morphology of GPC3-60 (a), GPC3-65 (b) or vector control (c) cells embedded in collagen I gels (final collagen I concentration of 2.3 mg/ml). Arrowheads indicate invasively growing tips. (D) R-cells grown in 3D collagen I gels. Morphology of GPC3 (a) or vector control (b) cells embedded in collagen I gels (final collagen I concentration of 2.3 mg/ml).

Supplementary Files

This is a list of supplementary files associated with this preprint. Click to download.

- SupplementaryFigureGenderGPC31216.pdf
- SupplementaryFigureGenderGPC31216.pdf